Temporal structure in the light response of relay cells in the dorsal lateral geniculate nucleus of the cat

Klaus Funke and Florentin Wörgötter*

Institute of Physiology, Department of Neurophysiology, Ruhr-Universität Bochum, 44780 Bochum, Germany

1. The spike interval pattern during the light responses of 155 on- and 81 off-centre cells of the dorsal lateral geniculate nucleus (LGN) was studied in anaesthetized and paralysed cats by the use of a novel analysis. Temporally localized interval distributions were computed from a 100 ms time window, which was shifted along the time axis in 10 ms steps, resulting in a 90% overlap between two adjacent windows. For each step the interval distribution was computed inside the time window with 1 ms resolution, and plotted as a greyscale-coded pixel line orthogonal to the time axis. For visual stimulation, light or dark spots of different size and contrast were presented with different background illumination levels.

2. Two characteristic interval patterns were observed during the sustained response component of the cells. Mainly on-cells (77%) responded with multimodal interval distributions, resulting in elongated 'bands' in the 2-dimensional time window plots. In similar situations, the interval distributions for most (71%) off-cells were rather wide and featureless. In those cases where interval bands (i.e. multimodal interval distributions) were observed for off-cells (14%), they were always much wider than for the on-cells. This difference between the on- and off-cell population was independent of the background illumination and the contrast of the stimulus. Y on-cells also tended to produce wider interval bands than X on-cells.

3. For most stimulation situations the first interval band was centred around 6–9 ms, which has been called the *fundamental interval*; higher order bands are multiples thereof. The fundamental interval shifted towards larger sizes with decreasing stimulus contrast. Increasing stimulus size, on the other hand, resulted in a redistribution of the intervals into higher order bands, while at the same time the location of the fundamental interval remained largely unaffected. This was interpreted as an effect of the increasing surround inhibition at the geniculate level, by which individual retinal EPSPs were cancelled. A changing level of adaptation can result in a mixed shift/redistribution effect because of the changing stimulus contrast and changing level of tonic inhibition.

4. The occurrence of interval bands is not directly related to the shape of the autocorrelation function, which can be flat, weakly oscillatory or strongly oscillatory, regardless of the interval band pattern.

5. A simple computer model was devised to account for the observed cell behaviour. The model is highly robust against parameter variations. Convergence of the model LGN cells onto cortical target cells yielded, in almost all cases, oscillations in the 30–90 Hz range.

Viewing a stationary image has been regarded as an analysis of local contrasts by a 2-dimensional neural network that performs a spatial filtering process. The spatial profile of illumination is finally encoded in the spatial distribution of activity, with the discharge rate coding for local intensity (Adelson & Bergen, 1991). This simple but intuitive model has been drastically altered over the past few years, during which increasing evidence has accumulated for the importance of temporal processes, even for the analysis of *stationary* visual scenes. In this context, the suggestion that is probably most frequently cited is that certain oscillatory spiking patterns of cortical cells could subserve synchronization processes. Coherent activity in a cell assembly has been assumed to be necessary for feature

* To whom correspondence should be addressed.

linking or foreground–background discrimination (von der Malsburg, 1981; Eckhorn *et al.* 1988; Gray, König, Engel & Singer, 1989). Synchronization has long been known to be one of the central mechanisms for the information transmission between different cortical areas, if only for the reason of the high divergence and convergence in the connectivity of cortical cells (Abeles, 1982). This divergence–convergence pattern makes spatial *and* temporal summation (i.e. synchronization) necessary, without which most incoming spikes would elicit only subthreshold voltage changes in the membrane of the target cell (van de Grind, Koenderink, van der Heyde, Landman & Bouman, 1971; Abeles, 1982). Temporal patterns, such as oscillations, could thus be the driving force for a synchronization that would have to be maintained over at least several hundreds of milliseconds to allow for higher level pattern recognition (Sompolinsky, Golomb & Kleinfeld, 1990).

Many studies have demonstrated a temporally structured activity in the visual cortex (Eckhorn *et al.* 1988; Gray *et al.* 1989; McClurkin, Optican, Richmond & Gawne, 1991*b*). In the cat and rabbit, rhythmic activity was also found in the retina by some investigators (Laufer & Verzeano, 1967; Ariel, Daw & Rader, 1983), while others failed to show oscillations (Kuffler, FitzHugh & Barlow, 1957; Rodieck, 1967; Troy & Robson, 1992). Rodieck (1967) noted that cells with a narrow interspike interval distribution would unequivocally produce an oscillatory spiking pattern even in the case of statistical independence between adjacent intervals (Moore, Perkel & Segundo, 1966). Therefore, the transition between oscillatory and non-oscillatory retinal cells could be gradual and the cell behaviour might actually change with the stimulus even for an individual cell.

Also in the dorsal lateral geniculate nucleus (LGN) a recent study was able to demonstrate oscillations (Ghose & Freeman, 1992). These results suggest that at least a proportion of the oscillatory activity in the cortex relies on the temporal patterns occurring in the input signals and it seems as if the lower visual centres could contribute significantly to the temporal structure of the spiking pattern in the visual cortex (Bringuier, Fregnac, Debanne, Shulz & Baranyi, 1992).

An oscillation can be regarded as a relatively simple temporal pattern, because it can be described by only two parameters: amplitude and frequency. If a reference point in time is given, the phase will be a third parameter. In addition, oscillations are rather easily accessible, because spike trains can be analysed by means of Fourier methods (viz. correlation functions) and, therefore, most studies cited above have focused on this topic. A temporal code restricted to two or three parameters could be too sparse for general use in the visual system. The question, therefore, arises of whether there are temporal features other than oscillations in the spike trains of cortical or subcortical cells and to what degree such patterns could be used for information processing.

Several studies have made remarkable advances concerning this question. For example, Dayhoff & Gerstein (1983) showed by multiunit recording that repetitive patterns of individual spikes occur in different cortical cells, which could be indicative of dynamic cell-assembly formation. Furthermore, it is known from studies analysing the principal components of LGN cell responses, that even in non-oscillatory cells a significant amount of information could be carried in the temporal structure of the spike trains (McClurkin, Gawne, Optican & Richmond, 1991*a*; McClurkin *et al.* 1991*b*) and that cells might switch between two transmission modes that show a different temporal type of activity (Funke & Eysel, 1992; Kaplan, Mukherjee & Shapley, 1993).

The LGN, therefore, may play a significant role in the initiation of temporal response features of cortical cells (see also Bringuier *et al.* 1992). It is also known that the LGN acts as an 'intelligent gateway' by integrating modulatory influences from different parts of the brain (arousal centres and oculomotor regions of the brainstem and visual cortex) to regulate the information flow from retina to cortex (see Singer, 1977). This raised our interest to investigate the temporal structure of LGN spike trains for its importance in such a gating function. Gating, compared with other more complex steps in information processing, is a rather basic mechanism and so we expected that any temporal structure possibly involved in such a process would also be relatively simple. Individual spiking patterns (e.g. groups of action potentials) might already be too sophisticated and too noisy to underlie such a basic task; therefore, we decided to analyse the interval distribution of LGN spike trains more closely. To this end, we have designed a simple method, which shows the transient changes in the interspike interval distributions following stimulation.

Similar to a sonogram in acoustics, where power spectra are computed in small, shifted time windows, in this study we compute 'intervalograms' as a multitude of overlapping and temporally local interval distributions of LGN cell responses. It should be noted that this method can be applied to any sequence of spikes and, in particular, to spike trains containing repetitive but noisy patterns, which would be disguised using Fourier methods. We will show in this way that LGN cells prefer certain firing intervals and multiples thereof. This feature is markedly pronounced in on-cells but not in off-cells, so that a distinct difference in the temporal firing pattern of these two subsystems is given. The observed time structure is probably generated as a result of inhibitory intra-LGN processing. Such a mechanism provides a very efficient means of down-regulating the firing frequency during non-optimal stimuli, possibly subserving a gating mechanism like that discussed

above. At the same time it could facilitate synchronization in the cortical target cells during states of high activity. Simulations also show that this pattern will unequivocally generate oscillations in the 30–90 Hz range in the cortical target cells, which could indicate the importance of the LGN in the generation of cortical spiking sequences.

METHODS

Anaesthesia and general procedures

Experiments were carried out on fifteen adult cats of either sex (body weight, 2·5–4·0 kg). Surgeries to enable infusion and artificial respiration were performed under anaesthesia induced with ketamine hydrochloride (20–25 mg kg^{-1}, I.M.; Ketanest; Parke-Davies, Berlin, Germany) and xylazine (1 mg kg^{-1}, I.M.; Rompun; Bayer, Leverkusen, Germany). While still under ketamine–xylazine anaesthesia, the cat was paralysed by alcuronium chloride infusion (0·15 mg kg^{-1} h^{-1}; Alloferin 10; Hoffmann-La Roche, Germany) through a cannula in the femoral artery, and artificial ventilation with N_2O–O_2 (70:30) and halothane (0·2–0·4%; Fluothane; ICI-Pharma, Germany) was started immediately. Further surgeries (e.g. craniotomy) were performed during this state of mixed ketamine–xylazine + N_2O–O_2–halothane anaesthesia. Craniotomies were performed for epidural EEG monitoring (silver ball electrode, area 17), for placing two concentric, bipolar stimulation electrodes bilateral to the optic chiasm, and for vertical access to the lateral geniculate nucleus. Adequacy of anaesthesia was ensured by continuously and semi-automatically monitoring the blood pressure and the EEG activity. The level of anaesthetic was increased (0·8–1·0% halothane) as soon as an increase in blood pressure or a desynchronization of EEG activity was observed. During normal recording sessions such changes were almost never observed, which indicated a sufficient level of anaesthesia. Any potentially noxious manipulation of the animal was only performed during an increased level of anaesthesia (0·8–1·0% halothane) with particularly careful control of blood pressure and EEG.

During recordings anaesthesia was maintained with N_2O–O_2 (70:30) and halothane (0·2–0·4%). The local anaesthetic xylocaine (2% gel; Astra Chemicals, Wedel, Germany) was applied to all wound margins and pressure points. The end-expiratory partial pressure of CO_2 was kept at about 3·8%, the body temperature was 38·0 °C, and the mean arterial blood pressure was maintained above 90 mmHg throughout the experiments. Atropine sulphate (1%; Atropin-Pos; Ursapharm, Bübingen, Germany) and phenylephrine hydrochloride (5%; Neosynephrin-Pos; Ursapharm) were applied topically for mydriasis and retraction of the nictitating membranes. The corneae were protected with zero power contact lenses and the optics were corrected with spectacle lenses of 5–7 dioptres to focus the screen image on the retinal surface.

Recordings, visual stimulation and data collection

Extracellular recordings were made in thirteen experiments with single-barrelled glass pipettes filled with 3 M NaCl solution and with an outer tip diameter of 3–6 μm. In two experiments cells were recorded with glass-coated tungsten electrodes. Visual stimuli were generated by a Picasso cathode ray image generator (Innisfree, Cambridge, MA, USA) and presented on an oscilloscope screen (Tektronics 608; frame rate, 200 Hz) 0·28 m in front of the cat's eyes. Light or dark spots of variable diameter (0·2–5 deg) were used to elicit receptive field centre or centre–surround responses and large-field moving gratings (24 × 20 deg; spatial frequency, 0·25–0·5 cycles deg^{-1}; velocity, 5–20 deg s^{-1}) were used to stimulate the far periphery of the receptive field. Most cells were also tested with moving light or dark bars (0·5 × 10·0 deg) at velocities ranging between 1 and 20 deg s^{-1}. In all but one control experiment background room illumination was 0·1 cd m^{-2}. For the on-cells light spots were flashed either on a dark background (0·1 cd m^{-2}, spot: max. 10·0 cd m^{-2}) or on a background of intermediate illumination (2·0 cd m^{-2}; spot: max. 20·0 cd m^{-2}). For the off-cells either a light spot of 10·0 cd m^{-2} was switched off to the dark background level or dark spots (0·1 cd m^{-2}) were presented on the intermediate background illumination. In one control experiment background room and screen illumination were varied widely (between 0·01 and 10·0 cd m^{-2}; step, 1 log unit) and cells were allowed to adapt for up to 30 min so that the response variability could also be tested as a function of the level of adaptation. Contrast between the spot and the screen background was varied between 0·05 and 0·9($[L_{bright} - L_{dark}]/[L_{bright} + L_{dark}]$), where L means luminance. Most cells were tested at least with a contrast of 0·2 in addition to 0·9. Retinal illumination was in a range of 0·89–3·19 log cat trolands.

After conventional electronic amplification, analog single unit action potentials were selected through a window discriminator (Model 121; WPI Instruments, New Haven, CT, USA), converted to −5 V pulses and fed on-line via a laboratory interface (Model 1401; Cambridge Electronic Design, Cambridge, UK) into a conventional personal computer. Each record contained between 100 and 500 sweeps of stimulus presentation (200 ms stimulus off, 800 ms on, 800 ms off).

Cell classification

Based on response latency to electrical stimulation of the optic chiasm and/or the spatial and temporal characteristics of their receptive fields, geniculate relay cells were classified as X- or Y-type (see Eysel, Grüsser & Hoffmann, 1979). All cells included in this study were of the non-lagged type (Mastronarde, 1987).

Data analysis

Commonly, an interspike interval distribution is computed by counting how often intervals of certain lengths occur between two adjacent spikes. Usually the interval length is binned in 1 ms steps and the distribution is computed for the whole duration of the record. To allow for an analysis that is more localized in time, we have devised a novel method for the analysis of interval distributions (Fig. 1).

In Fig. 1*A* (not to scale) the time axis is plotted downwards. Along the time axis a peristimulus time histogram (PSTH) was calculated with an initial temporal resolution of 1 ms per bin and is finally shown in the figures with a temporal resolution of 10 ms per bin (Fig. 1*A* and *B*). On a second axis the interval distribution is plotted horizontally and a conventional interspike interval histogram (dubbed 'summed interval histogram') is shown above for comparison (resolution, 1 ms per bin). A temporally local interval distribution ('time window INTH', Fig. 1*A*) is then computed in a small time window of 100 ms length, also with a resolution of 1 ms per bin. The time window INTH is plotted as a grey-scaled pixel line to the right, centred with respect to the centre of the time window. The window is then shifted 10 ms along the time axis, resulting in a 90% overlap between adjacent windows, and the next time window INTH is computed and

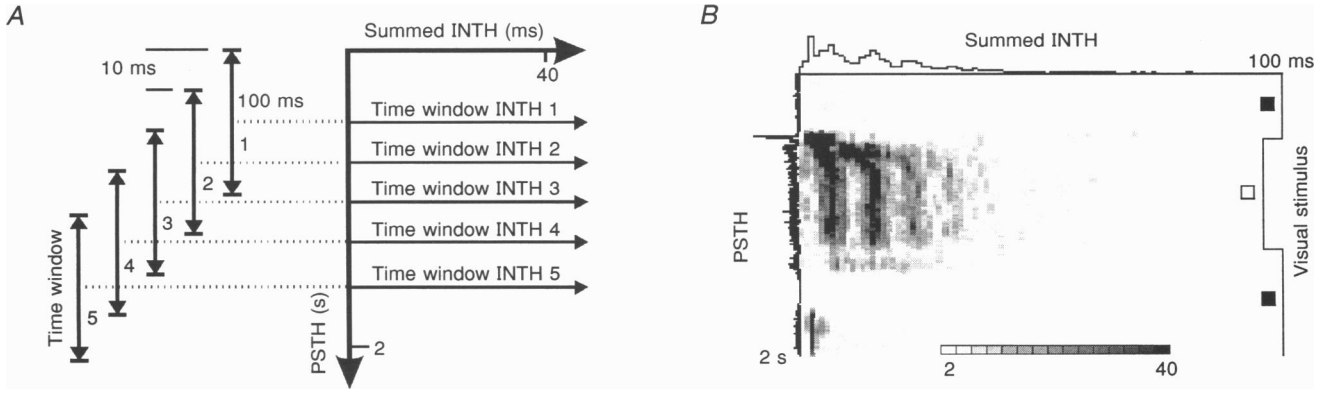

Figure 1. Schematic (*A*) and original (*B*) drawing of an 'intervalogram'

The intervalogram demonstrates the dynamic changes in the distribution of spike intervals during a visual response elicited by a spot of light projected onto the centre of a geniculate receptive field. A conventional peristimulus time histogram (PSTH) is plotted along the vertical time axis and shows the mean firing rate during the visual response. For a small time window of 100 ms an interval distribution is computed and plotted as a grey-scaled horizontal pixel line centred with respect to the time window. Then the time window is shifted by 10 ms along the time axis and a new interval distribution is plotted as the next pixel line. The regular interval histogram above (Summed INTH) represents the sum of all pixel lines. The temporal resolution of the time axis (vertical axis) is 10 ms; that of the INTH horizontal axis is 1 ms. As demonstrated in *B*, the interval distribution during the tonic part of the light response is not a continuous Poisson- or γ-like distribution, but a multimodal distribution, which appears as a banded structure in the intervalogram.

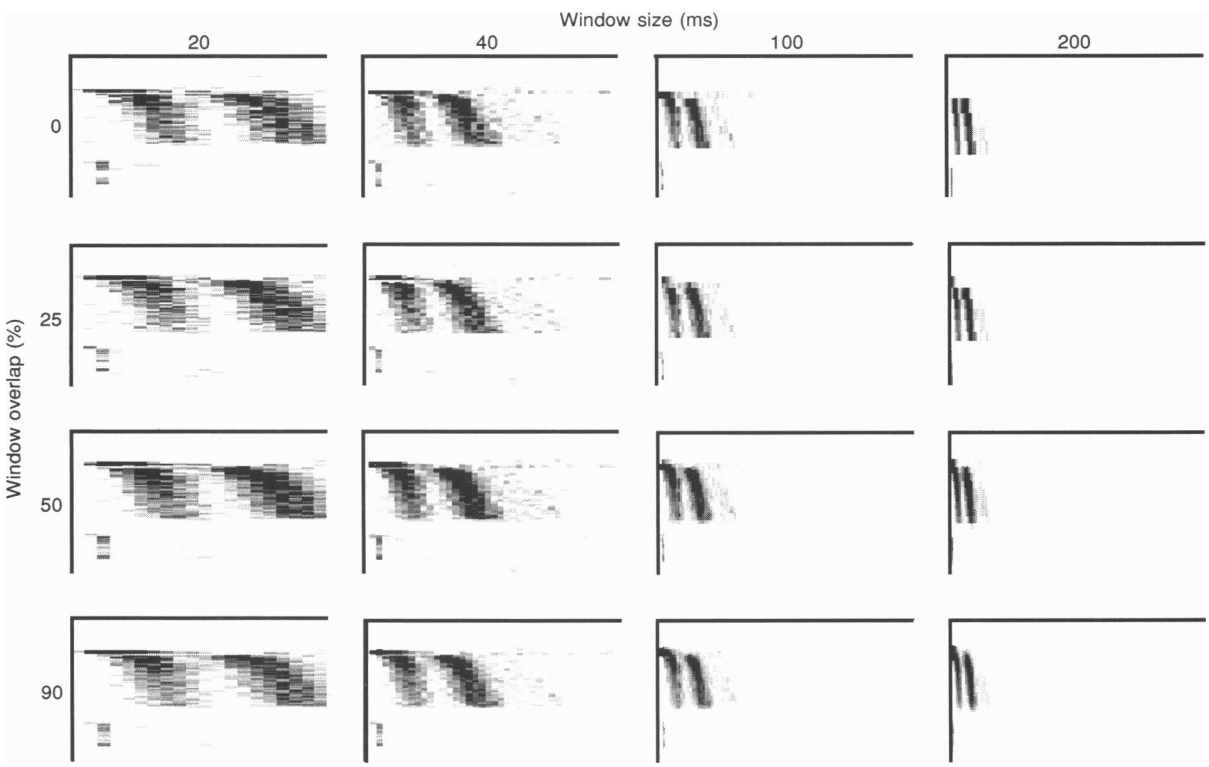

Figure 2. Comparison of intervalograms for an X on-cell using different parameters for window size and window overlap

Absolute values for the greyscales of the diagrams are as follows. Top two rows: 10, 12, 30, 50; third row: 12, 20, 50, 80; bottom row: 15, 25, 60, 100. All units are *N*/bin. No differences other than scaling effects are visible concerning the band-shaped pattern.

plotted. This process is repeated until the end of the PSTH is reached. We call the complete diagram obtained in this way an 'intervalogram'. In general, intervalograms show the progressive changes in the interval distributions during stimulation. The intervalogram of the X on-cell shown in Fig. 1*B* displays two to three distinct tilted bands, which reflect a multimodal interval distribution, which is also vaguely indicated in the summed interval histogram (top).

Figure 2 shows that the size and the shape of the interval bands remain totally unaffected if different parameters are chosen for the window size and the overlap between the windows. The distortion of the diagrams that occurs is only a scaling effect, because the number of pixels decreases from the top right of the figure to the bottom left. On the other hand, the number of intervals found in a given time window increases from the top left to the bottom right and, therefore, the absolute scale (maximum number of intervals, see legend) of the diagrams has been set to identical grey levels to make them better comparable.

It is obvious that a change in the window overlap cannot result in any change of the banded pattern, because each individual pixel line represents nothing but a conventional interval distribution computed from the whole record but at a given starting point in time. The intervalogram, therefore, makes features of the interval distributions better visible without any artificial interference with the interval data.

The window size could in principle be critical, but only if the individual interval distributions changed on a time scale faster than 100 ms, e.g. due to adaptation, which was not observed for the tonic response component in any cell that we recorded. Alternatively, the window size could affect the data if long spiking patterns of some interesting shape existed in the trains, which was also never observed. One hundred milliseconds window size was finally chosen because almost all interspike intervals of LGN cells fell in the range of 2–50 ms, so 100 ms is a good compromise, in which the longer intervals were not missed too often.

In some cases conventional auto- or cross-correlation diagrams were also computed (Figs 9, 12 and 13).

RESULTS

Stimulus variations and cell types

Figures 1*B* and 2 show that some LGN cells produce a structured interval pattern, resulting in multiple interval bands that reflect a bi- or multimodal distribution. We have tested this feature for a total of 236 LGN cells of the non-lagged type (see statistics below), with varying stimuli but mostly with flashing dots. Figure 3 shows the behaviour of a typical X on-cell for moving and flashing dot and bar stimuli. As soon as the stimulus illumination changes slowly, or not at all, a more or less sustained cell response is obtained. During this period, interval bands are normally observed. Note that in most of the cases shown, the multimodal interval distribution is better discernible in the intervalogram than in the summed interval histogram plotted above. For the flashing dot, two response phases can be distinguished (Fig. 3*A* and *B*). Immediately after stimulus onset, a high-frequency phasic response with interspike intervals between 2–4 ms occurs. During this short burst-like activity no interval bands are observed. The phasic response is followed by sustained activity of the cell, which leads to the expression of two to four interval bands. The first interval band is centred around 7 ms, which will be called the 'fundamental interval'. The other bands will be called the 'higher order bands' and reflect longer intervals, i.e. lower firing frequency. Each following band is a multiple of the fundamental. In the cells where bands occur, we could observe a maximum of five or sometimes six of them. Since higher order bands reflect longer intervals, fewer of them can occur in a given time. Therefore, we cannot rule out the possibility that even more bands might be observed during a very long stimulus or with a higher number of stimulus repetitions.

In this and most of the following figures, the bands have a curved appearance which, we believe, is the result of slow adaptation effects to the stimulus. Note that this adaptation is much slower than the time window size (100 ms) used for the intervalograms.

Figure 4 shows typical intervalograms for X and Y on-cells (Fig. 4*A* and *B*) as well as X and Y off-cells (Fig. 4*C* and *D*) stimulated with a flashing dot. The insets are conventional interspike interval histograms computed by averaging five adjacent time window INTHs (i.e. averaging 5 adjacent pixel lines). They were computed next to the intersection lines cutting through the intervalograms at about 800 ms. While, for the on-cells, pronounced interval bands occur, only wide and unimodal distributions are observed for the off-cells. Y-cells, in general, have the tendency to fire less regularly and with a somewhat longer fundamental interval than X-cells, which widens the distribution and fills in the gaps between the bands in Fig. 4*B*.

Cell statistics

The different behaviour of on- and off-cells could be confirmed statistically. In the first step we will use a rather qualitative statistical grouping scheme, because the individual cells were tested with quite different stimuli, which were adjusted to elicit bands optimally, if bands could be elicited at all. Therefore, only a qualitative scheme allows pooling of all cells regardless of cell class and individual stimulus situation. Figure 5*A* shows the distribution of cells that produce sharp interval bands (++), weak or broad bands (+−) or no bands at all (−−). The grouping was performed by determining the width at half-height of only the *leftmost* peak of activity in the intervalogram, which represents the fundamental interval length (see Fig. 4 and legends for details). All cells included in these groups were tested with different stimulus sizes and most of them also with varying stimulus contrast and under different levels of adaptation. On-cells, in general, respond with much sharper interval bands than off-cells. Most of the off-cells are indeed able to produce some kind of band-shaped pattern under optimal stimulus conditions. Those bands, however, are very broad and, in many cases, melt into a single wide blob of intervals. Very few off-cells were found that show sharp bands. The occurrence

probability and/or the shape of the bands was very little affected in the off-cells if we chose a bright stimulus that was switched off or a dark stimulus that was switched on.

Figure 5*B* shows the *maximal number* of bands found in cells belonging to the different groups in Fig. 5*A* (see legend for details). Only if the leftmost peak in the intervalogram was narrow (++ and +− groups), did we find multiple bands. If the leftmost peak was broad (−−), the interval distributions looked Poisson-like, with one broad peak in all cases but one, which was a single X on-cell that showed a distribution with two broad peaks (no real bands as defined by the width at half-height criterion). In a total of 5·7% of off-cells (4 out of 70 cases; 1 band in ++ group) we found a single sharp band. In these cases it cannot be ruled out that our stimulation might have been inappropriate to elicit more bands. Multiple bands were displayed by only 18·6% (13/70) of the off-cells; the remaining 75·7% did not show even a single clear band. For the on-cells, on the other hand, we have 13·3% uncertain cases (20 out of 150; 1 band in ++ group), 63·3% (95/150) cases with clear multiple bands and only 23·3% (35/150) recordings that did not show a clear band. If we discard the uncertain cases, the difference between on- and off-cells concerning the tendency to display multiple bands or not is significant at the 1% level using the χ^2 test.

Figure 5*C–F* shows summary diagrams for the interval distributions of the different cell classes taken from a cross-section of the intervalograms at 800 ms. Here we show the averaged interval distributions for only those cells that were analysed with almost the same stimulus conditions: a light (or dark) spot of high contrast to background covering the whole centre and a small fraction of the receptive field

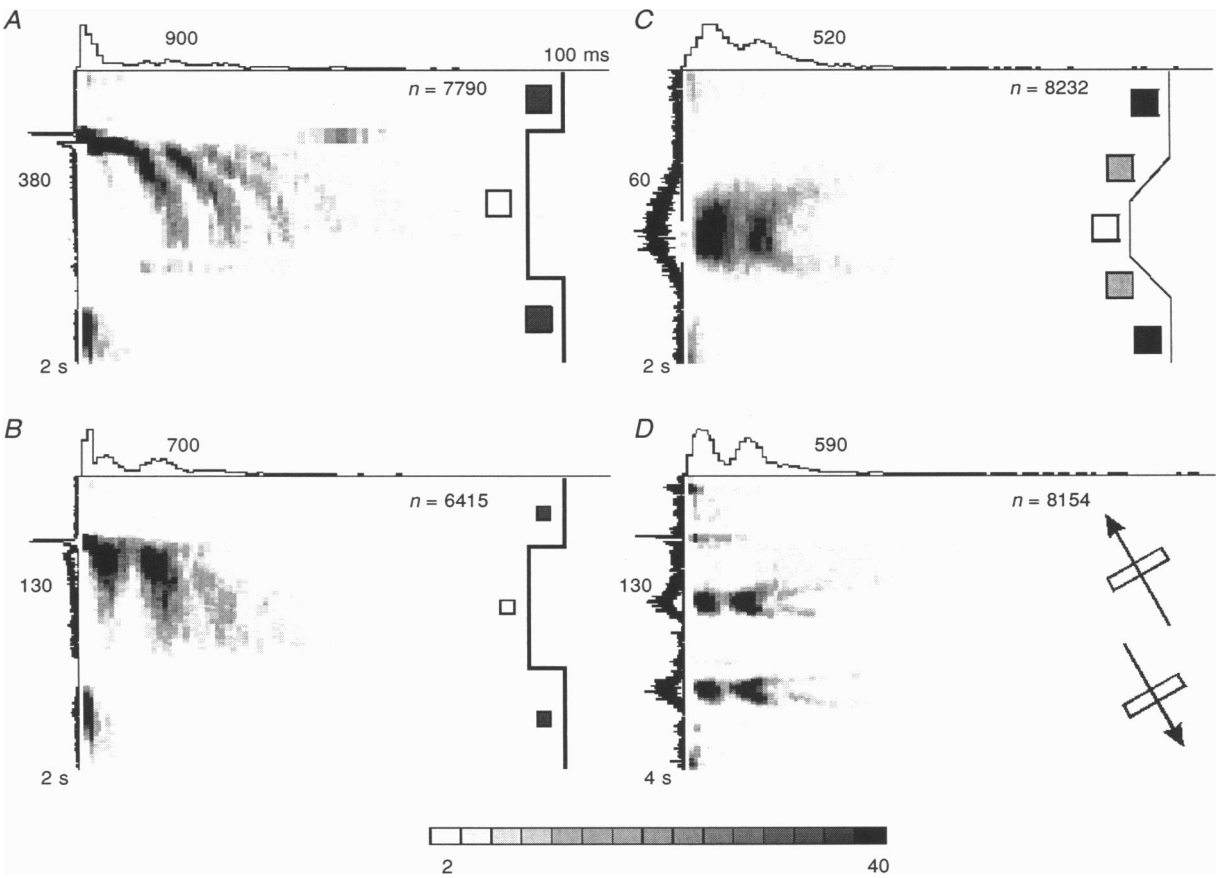

Figure 3. Intervalograms obtained from an X on-cell during four different stimulus presentations

Stimulus presentations were: rectangular modulation of light intensity (flash) of a large (1 deg; *A*) or a small (0·3 deg; *B*) spot; ramp-like changing intensity of a light spot (1 deg; *C*); and movement (5 deg s^{-1}) of a light bar (0·5 × 5 deg) across the receptive field (*D*). All stimulus presentations have almost 100% contrast modulation. Multimodal interval distributions are obtained with all stimulus types. The moving bar (*D*) causes dynamic changes in the interval distribution very similar to those obtained with ramp-like modulation of light intensity inside the receptive field (*C*). The histograms are obtained from 100 stimulus repetitions; numbers give either the value of the maximal bin in the INTH and PSTH, or the total number, indicated by *n*, of intervals included in the intervalogram.

surround (spot, 0·3–1·0 deg for X-cells; 0·5–2 deg for Y-cells). The indicated number (n) of cells was averaged for each individual diagram. This allowed us to depict the characteristic shape of the interval distributions, although there is a smoothing effect owing to the response variability of the different cells in each class, i.e. the interval bands of some X on-cells were sharp, but at a position slightly different compared with other cells in this class. Interval counts are normalized with respect to the cell number, which allows a judgement of the total activity. As expected, only on-cells show bands, but the second band is reduced to a shoulder for the Y on-class. The less pronounced separation between the bands already visible in the example of Fig. 4*B* together with the response variability certainly contributes to this effect. Not even a shoulder, however, is visible for the off-cells, although the analysis includes a few cells (3 in Fig. 5*E* and 1 in Fig. 5*F*) that actually showed multiple bands. The diagrams look similar to those of Fig. 4*C* and *D*, but the distribution is much broader. Some off-cells also generate very short spike intervals in the range of 2–4 ms, which is visible as the small early peaks in the inset INTHs of Fig. 4*C* and *D*. This 'burst-like' activity during the tonic light response was not taken as the fundamental interval, since it seems to be an intrinsic spike-generating mechanism different from the generation of single action potentials.

Influence of stimulus size and contrast

Is the multimodal interval pattern generated in the retina or does it result from intra-LGN processing? The higher order bands are always multiples of the fundamental interval. Since a single retinal spike has a strong probability of firing the target relay cell (see Mastronarde, 1987, 1992), it seems likely that the fundamental interval is already represented in the spike activity of the retinal ganglion cell that exerts a dominant input to an LGN cell. Failure of retinogeniculate transmission and/or inhibitory interactions inside the LGN would cancel some spikes, thereby leading

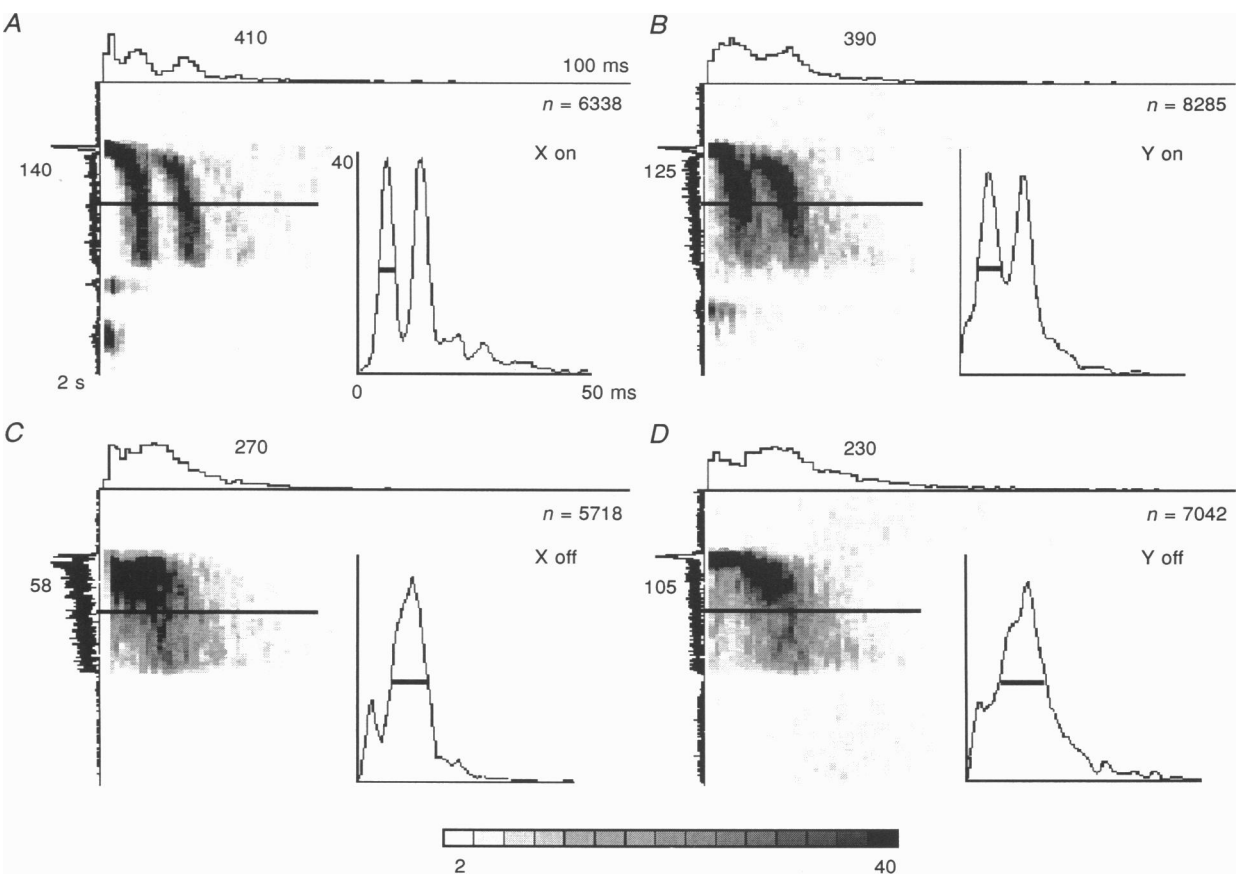

Figure 4. Intervalograms typical for the 4 different relay cell types of the geniculate A-layers
Insets show conventional INTHs calculated from the averaged values of five adjacent pixel lines from the tonic response at position 800 ms on the time axis (indicated by the horizontal line). Most often X on- (*A*) but also Y on- (*B*) cells show two or more separate interval bands or peaks; X off- (*C*) or Y off- (*D*) cells generate only broad and unimodal interval distributions. The off-cells have been stimulated with a bright spot that was switched off to background level (see Methods for illumination levels used). The widths at half-height of the interval peaks (thick line in the inset INTHs) were taken to classify cells as shown in Fig. 5. Stimulation was by a light spot of 1 deg and 100% contrast modulation in all cases.

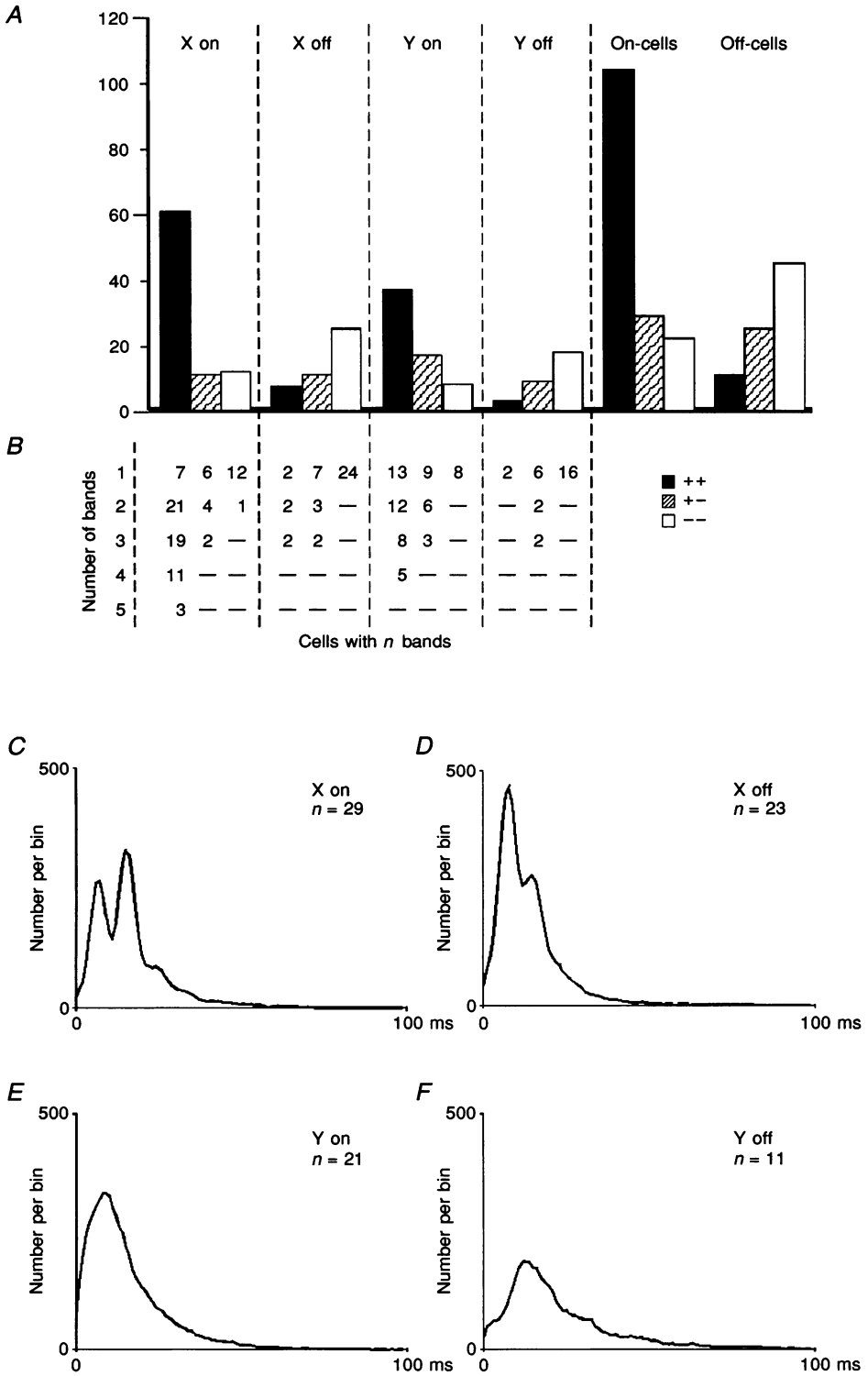

Figure 5. Cell type statistics

A, the number of different relay cell types showing rather sharp interval bands (++), broad and diffuse bands (+−) or no real interval band at all (−−). Classification was related to the width of the *leftmost* clear peak of the interval distribution at half-height at 800 ms, as in Fig. 4. (++), width at half-height $\leqslant$ 4 ms; (+−), width at half-height $>$ 4 ms and $<$ 9 ms; and (−−), width at half-height $\geqslant$ 9 ms or Poisson-like distribution. For typical examples of (++) see Figs 4*A*, 8*A*, 10*A* and 13*A*; for (+−) see Figs 4*B* and 8*B* and *D*; and for (−−) see Figs 7*D–F* and 10*C* and *D*. *B*, maximal number of bands observed in the different cells. Numbers reflect the count of cells with 1, 2,...5 bands. Each cell is only listed once in the highest group that applies. Bands above five were usually too faint to be accounted for. A band was counted if it occurred as a multiple of the fundamental and if the averaged activity in the gap

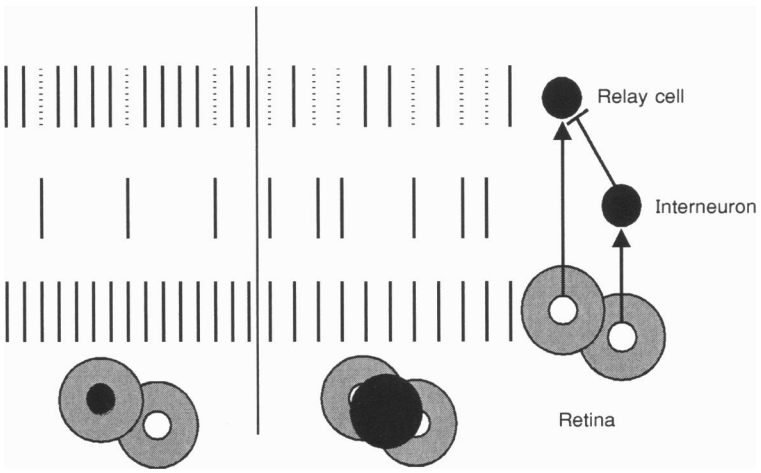

Figure 6. Simple qualitative model of a retinogeniculate connection scheme (to the right) that is sufficient to produce multiple interval bands in a geniculate relay cell

Receptive fields of retinal ganglion cells are drawn as discs with a white centre and a shaded surround. Sustained stimulation with a light spot (black discs) induces a very regular firing in the retinal ganglion cell that is directly linked to the relay cell (bottom row; black bars represent single spikes). The mean firing rate of the ganglion cell changes little with increasing stimulus size (compare left and middle column). Without inhibition a one-to-one transmission by the LGN relay cell is assumed (top row). During an inhibitory input (middle row) individual spikes are blanked out (dashed lines in top row) and multiples of the fundamental interval are obtained in this way. The number of fundamental intervals is strongly reduced and the number of multiples dominates when the inhibitory input is increased by stimulation of the ganglion cell that belongs to the inhibitory surround of the geniculate receptive field. The scheme to the right gives an example of an inhibition of the feedforward type; a feedback inhibitory connection would lead to the same results.

to the higher order intervals (Fig. 6). We will present two lines of evidence supporting the suggestion that inhibition could be involved. First, we will discuss stimulus-induced effects predictable from this assumption and, second, we will show simultaneous recordings from LGN cells and their retinal prepotentials.

Surround inhibition increases with increasing dot size. This effect is much more pronounced in the LGN than in the retina (Sillito & Kemp, 1983; Cleland & Lee, 1985). If our assumption holds, then an increase in stimulus size should result in a redistribution of the intervals into higher order bands, because more retinal spikes will be cancelled during

---

along the band exceeded the averaged activity in the gap between this band and the adjacent band to the left by at least 50%. To be able to compute this average, we fitted the curved shape of the bands along their centre by an arbitrary, multi-exponential function. The actual equation does not matter; anything that fits the band will do. Intervals were then counted for the whole 'width' of each band along the graph of this fitting function. To define the width of a band, we divided the distance between each two adjacent graphs (i.e. the distance between the centres of two adjacent bands) into three equal regions. Thus, two regions are located close to either one or the other graph. These give the half-width of the respective bands. The central region was defined as the gap between the bands and was used for the control counts. Most of the on-cells show multiple bands, whereas off-cells fail to do so. *C–F*, also in the summary interval histograms of the 4 cell types (which are averaged from the number of cells indicated in the diagrams) the differences in the interval distributions between the groups are clearly visible. The interval peaks are somewhat broader than those of the insets of Fig. 4, which can be regarded as owing to the smoothing effect of averaging. The interval distributions were taken from a cross-section through the intervalograms at 800 ms. These statistics include only responses elicited with a stationary flashing spot stimulus. In *A* and *B* the responses of single cells to different spot sizes and contrasts were taken into account. For *C–F*, only cell responses obtained with almost identical stimulus situations were averaged; light or dark spots with almost 100% contrast to background covered the full centre and a fraction of the antagonistic surround in all cases (spot sizes: X-cells, 0·3–1·0 deg; Y-cells, 0·7–2·5 deg). These relatively large spot sizes usually elicited bands most reliably.

stimulation with a large, compared with a small stimulus. Exactly this effect is shown for an X on-cell in Fig. 7*A–C*. The fundamental interval remains at (almost) the same location (between 7 and 9 ms) for all stimulus conditions, but most intervals are redistributed into the higher order bands as soon as the stimulus size increases. In particular, for the largest stimulus (Fig. 7*C*) very few intervals are found in the first band, which contained about half the intervals during stimulation with the smallest stimulus. Similar redistribution effects were observed in *all* cells that showed interval bands. Most off-cells, on the other hand, did not show a consistent effect, except for a further widening of the unimodal interval distribution with decreasing firing rate (Fig. 7*D–F*).

Centre–surround interactions alter the inhibitory impact on the target cell while, on the other hand, a changing contrast of a small centre stimulus should not lead to any inhibition, but rather to a gradual shift in the firing frequency owing to the changing afferent input. Shifts towards longer intervals as soon as the stimulus contrast is reduced can be observed in the X and Y on-cells shown in Fig. 8. This effect is especially strong for the higher order bands, as a result of the multiplicative relation between fundamental and higher order intervals. The mostly unimodal interval distribution of off-cells also shifts following a contrast change (not shown).

Simultaneous recordings of prepotentials and LGN cells

There is electrophysiological and anatomical evidence that most LGN X-cells receive only one predominant retinal input (Kaplan, Purpura & Shapley, 1987; Mastronarde, 1987). In two experiments, we recorded the LGN cells with

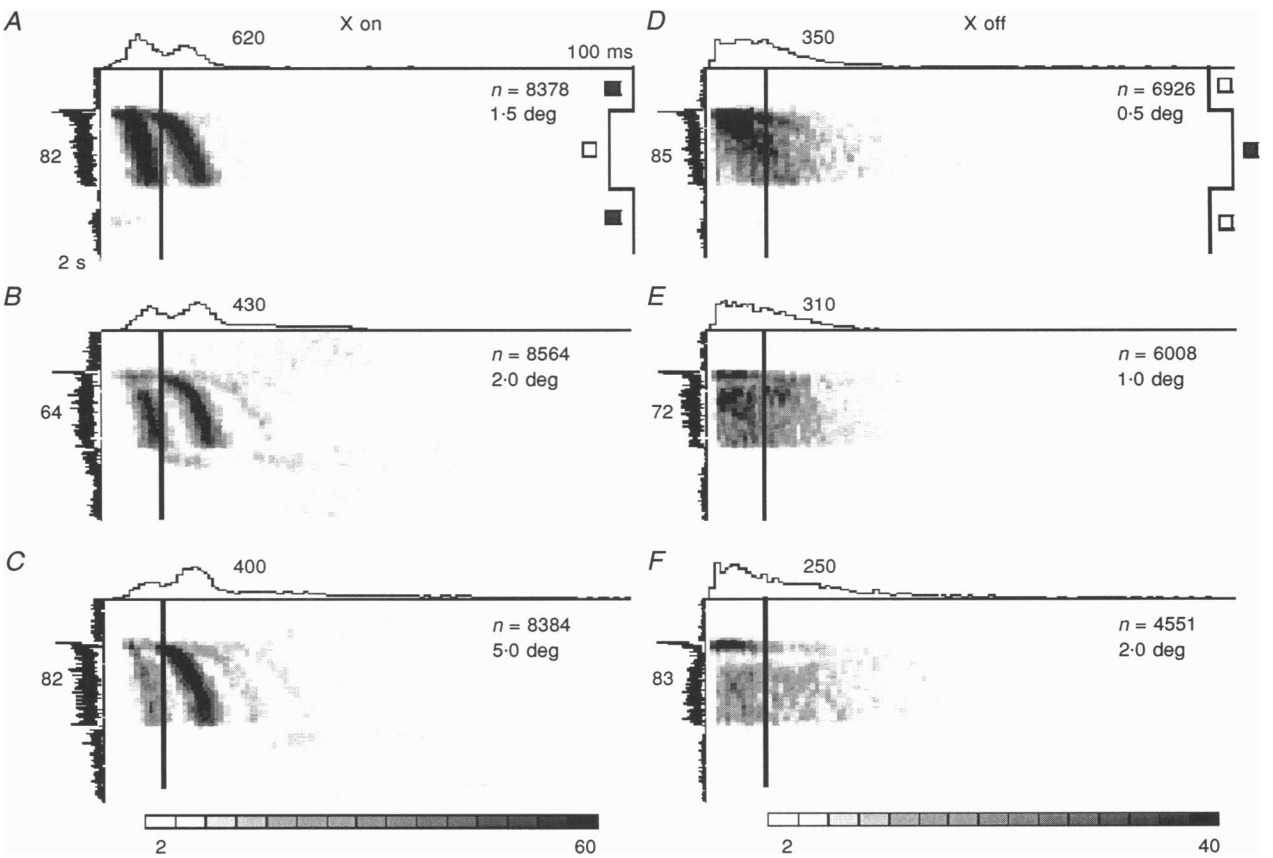

Figure 7. Effect of increasing stimulus size on the interval distribution shown for an X on-cell with interval bands (*A–C*) and an X off-cell with diffuse interval distribution (*D–F*)

The general pattern (banded/diffuse) is not affected by the size of the stimulus. In the case of the on-cell, the number of events in the first (fundamental) interval band decreases with increasing spot size and additional bands occur (*B*, 3 bands; *C*, 4 bands). The absolute location of the bands has not changed, as can easily be estimated from the reference line. The off-cell shows a more general reduction in the number of intervals over a wide range and the distribution is even more diffuse (*E* and *F*). The off-cell has been stimulated with a dark spot that appeared on a background of intermediate illumination level (see Methods for details). The activity shown in the PSTHs (left) and summed INTHs (top) is normalized to the individual peak response; numbers indicate the value of the maximal bin in the INTH and PSTH and the total number, indicated by *n*, of intervals included in the intervalograms. Contrast modulation is 50% for the on- and 100% for the off-cell.

glass-coated tungsten electrodes that are known for their capability to pick up electrotonic somatic potentials together with the spiking activity of the cell. Those somatic potentials, called prepotentials or S-potentials, have been attributed to the afferent input activity of the retinal cell that drives the LGN cell (Kaplan *et al.* 1987). Figure 9 shows two examples of simultaneously recorded LGN X on-cells and the corresponding prepotentials. The cross-correlograms in the insets of the intervalograms demonstrate a strong coupling between the two signals with a delay of less than 1 ms.

This can be seen also in the raster plots (Fig. 9*G* and *H*), where each double row represents the superimposed spike trains of prepotential and LGN cell. The short delay reflects the situation in which prepotential and spike are probably both recorded very close to the initiation site of the action potential. In one case, a flashing dot was used for stimulation (Fig. 9*A*, *B*, *E* and *G*); in the other case (Fig. 9*C*, *D*, *F* and *H*), illumination of the dot was changed with a ramp-shaped modulation function. Clearly, higher order interval bands are visible only for the LGN cells, but not for the prepotentials. A similar observation was made for all ten LGN–prepotential pairs that we recorded. In addition, three pairs of off-cells–prepotentials were recorded but, despite a lower rate of activity in the LGN cell, no difference in the general interval distribution was visible for those cases (data not shown).

Background illumination effects

Changing contrast or stimulus size results in two different and normally not superimposed effects of either a shift of the fundamental interval or a redistribution of intervals into other bands. Changing the background screen and/or room illumination while leaving the stimulus illumination at the same level results in a changed stimulus contrast while simultaneously altering the adaptation state of the cells. The latter effect can strongly modify the influence of the surround inhibition (Barlow & Levick, 1969). Consequently, we expected and found a mixed shift-redistribution effect of intervals during a change in the background illumination in the case of on-cells (Fig. 10*A* and *B*). An increase of background illumination results in a stronger maintained discharge that even leads to two faint bands

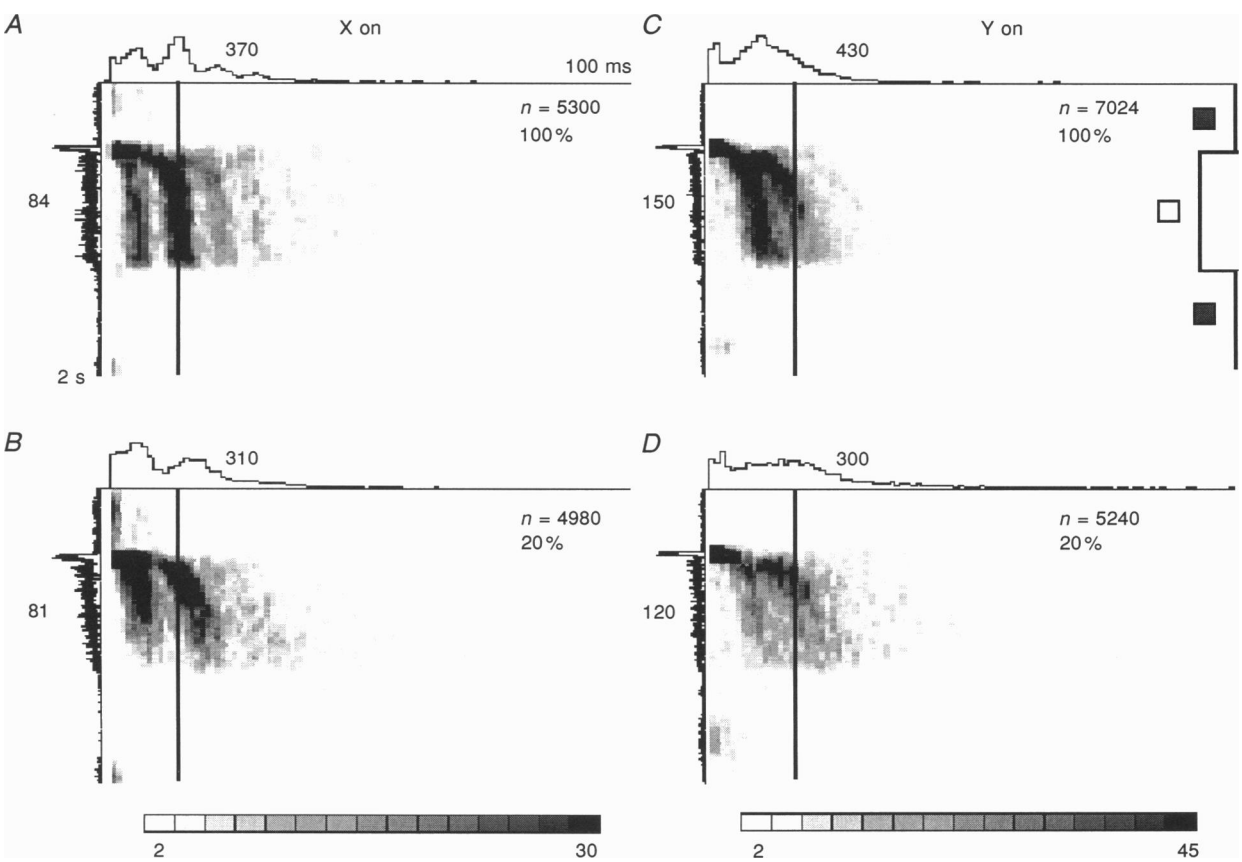

Figure 8. Effect of decreasing contrast on the intervalograms

As a counterpart to Fig. 7, the effect of a changing stimulus contrast is shown for an X on-cell in *A* and *B* (spot, 0·5 deg) and for an Y on-cell in *C* and *D* (spot, 1·0 deg). In both cases, a reduction of the stimulus contrast from 100 to 20% causes not only a general reduction in activity, but also a shift of the interval bands to the right (compare with location of the reference line), without a significant redistribution of intervals to the rightmost higher order bands.

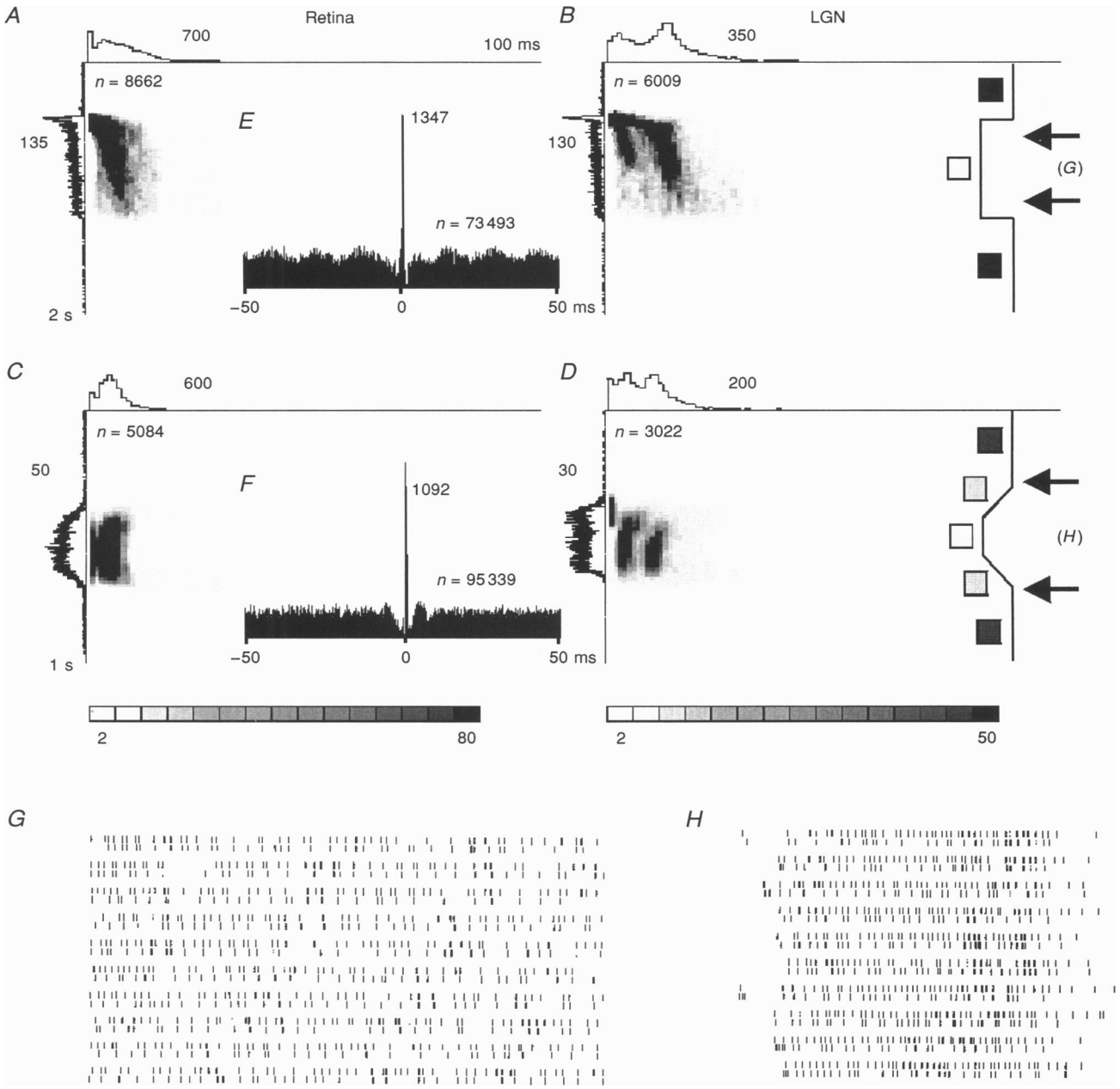

Figure 9. Intervalograms obtained from two different geniculate X on-cells (*B* and *D*) and from simultaneously recorded retinal prepotentials (*A* and *C*) together with raster plots of the prepotential and LGN spike trains (*G* and *H*)

In *A* and *B* the visual stimulus was a flashing dot (2·0 deg, 100%); in *C* and *D* (spot, 1·0 deg) a ramp-like modulation of light intensity was used (0–100% contrast). In both conditions, only the geniculate relay cells exhibit multiple interval bands; the retinal input generates only one band at the fundamental interval length. The cross-correlograms in *E* and *F* demonstrate the direct link between the retinal prepotential and the LGN cell (1 ms bins; n = number of spike correlations performed). Raster plots (*G* and *H*) show for 10 sweeps the prepotential activity (top sweep of pair) and the corresponding LGN cell activity (bottom sweep of pair). The period of the record from which the 10 activity sequences were taken is indicated by the arrows in the stimulus timing diagrams to the right of *B* and *D*. Not every prepotential elicits an LGN spike, while LGN spikes without prepotentials occur only very rarely.

containing rather long intervals. At the same time a redistribution of intervals into the second order band occurs during stimulation, probably owing to a change in the surround inhibition. As an additional effect, the stimulus contrast decreased, leading to a shift of the bands to the right. Most off-cells, again, do not show a distinctive behaviour (Fig. 10*C* and *D*). As expected, an increased background illumination enhances the contrast for the off-stimulus and results in a stronger response without altering the rather featureless intervalogram of this cell.

Periphery effects

Stimulation of the far periphery of the geniculate receptive field causes modulations in LGN activity known as the shift effect (Fischer & Krüger, 1974). When the cells had adapted to a stationary grating in the background, a subsequent continuous movement of the grating induced an inhibition of the tonic light response to the flashing spot in the centre of the receptive field in X-cells (Fig. 11*A* and *B*). Also this type of inhibition was characterized by a redistribution of intervals to the higher order bands, but in this case, the bands were also slightly shifted to the right. This observation indicates that the inhibition elicited from the far periphery acts in a slightly different way as compared to the inhibition from the antagonistic surround. In general, Y-cells were not inhibited by this stimulus (Fig. 11*C* and *D*).

Relations between band-shaped intervalograms and oscillatory spiking patterns

The question of whether a band-shaped intervalogram is associated with a more or less long lasting oscillatory pattern relies on the actual correlation length in the spike train. If rather sharp interval bands exist for a given cell and if they consist of long uninterrupted trains of intervals belonging

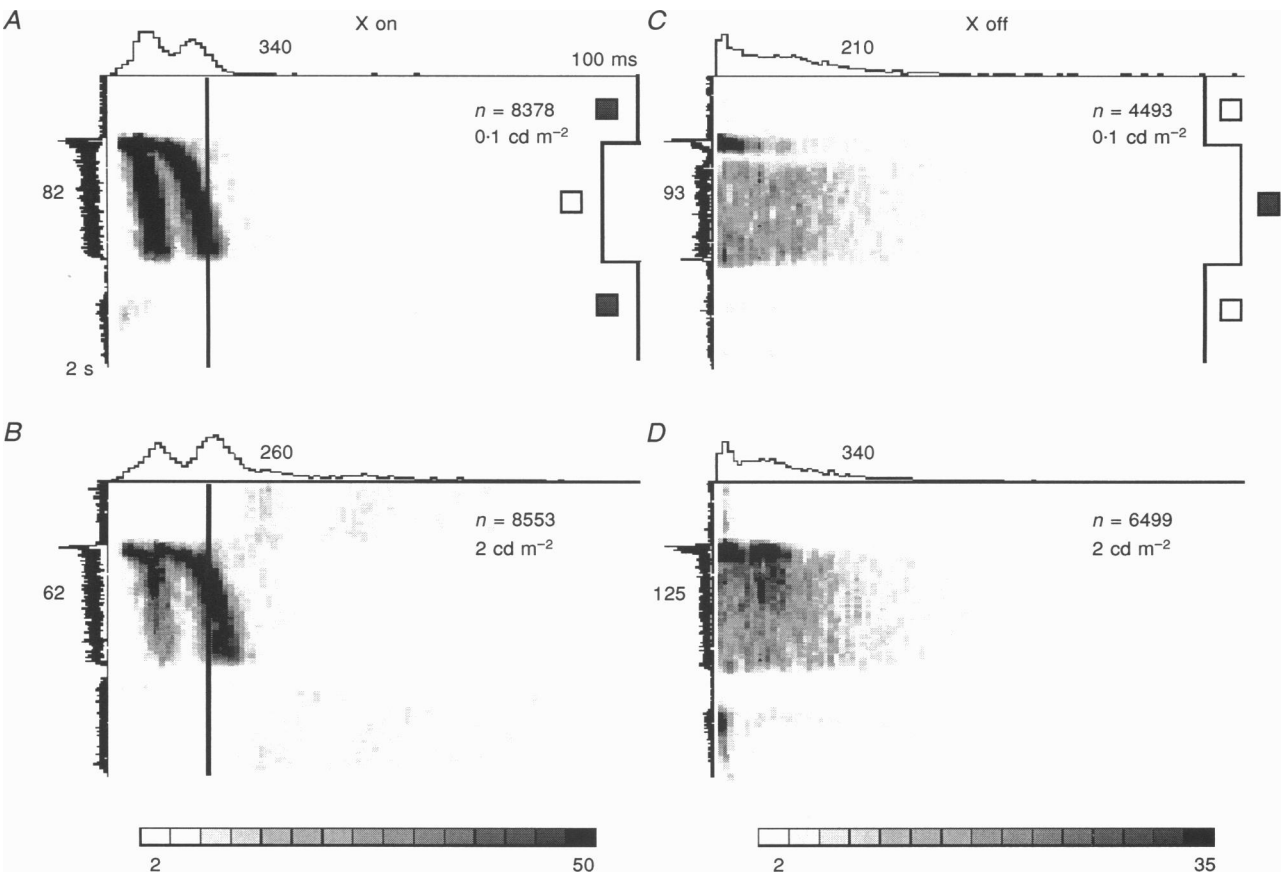

Figure 10. Effect of changing the adaptation level using different illumination levels of the background

The general interval pattern of both the X on-cell (*A* and *B*; banded) and the X off-cell (*C* and *D*; diffuse) is not affected by the two different adaptation levels. With an increase in background illumination, the light response of the on-cell is reduced and the 'spontaneous' activity during light-off is enhanced, which by itself generates weak interval bands (*B*). The effect on the interval bands during the tonic response is twofold: the bands shift slightly to the right and the number of intervals in the first band is reduced. As opposed to the on-cell, the tonic response of the off-cell increases with brighter illumination of the background, but the interval distribution is not altered. Spot size, 1·5 deg for the on-cell and 2·0 deg for the off-cell. Contrast modulation for each was 50%, achieved by using a light dot for the on- and a dark dot for the off-cell.

to either of the bands, then a strong oscillatory activity should arise (Fig. 12*A*). A strongly pronounced interval band pattern, however, does not allow the extrapolation of the occurrence of oscillations and, in many cases, only short repetitions were observed. The banded pattern in Fig. 12*A* and *C* is rather similar, with the exception of a different location of the fundamental interval. However, one cell shows long-lasting oscillations in the auto-correlogram (Fig. 12*B*), while the other cell does not show any oscillations at all (Fig. 12*D*). Most commonly observed are short-lasting reverberations in the autocorrelograms, such as those shown in Fig. 13 (3–7 peaks in the histograms).

Assessment of robustness: a simple computer simulation

The diagram in Fig. 6 suggests a very simple mechanism for the generation of the interval band pattern. In this section we will show that such a model and a simple extension of it will produce realistic interval patterns in simulated LGN relay cells and will generically lead to oscillations in a mimicked cortical cell. We will first present the simulation results and, in the Discussion, elaborate on the draw-backs of this simplified scheme.

First, it should be noted, however, that this model relies on the assumption of a one-to-one transmission between retina and LGN (see Fig. 6), for which there exists direct electrophysiological evidence (Kaplan *et al.* 1987; Mastronarde, 1987). For simplicity, we also assume only feedforward inhibitory connections. There are, however, no reasons why the results described below should critically depend on this feedforward connectivity. The model behaviour should be robust as long as the shape and distribution of the postsynaptic potentials remain within the required limits.

Thus, the most reductionistic model requires only feedforward connections and needs just four parameter sets for the input cells to the LGN: (1) EPSP characteristic of

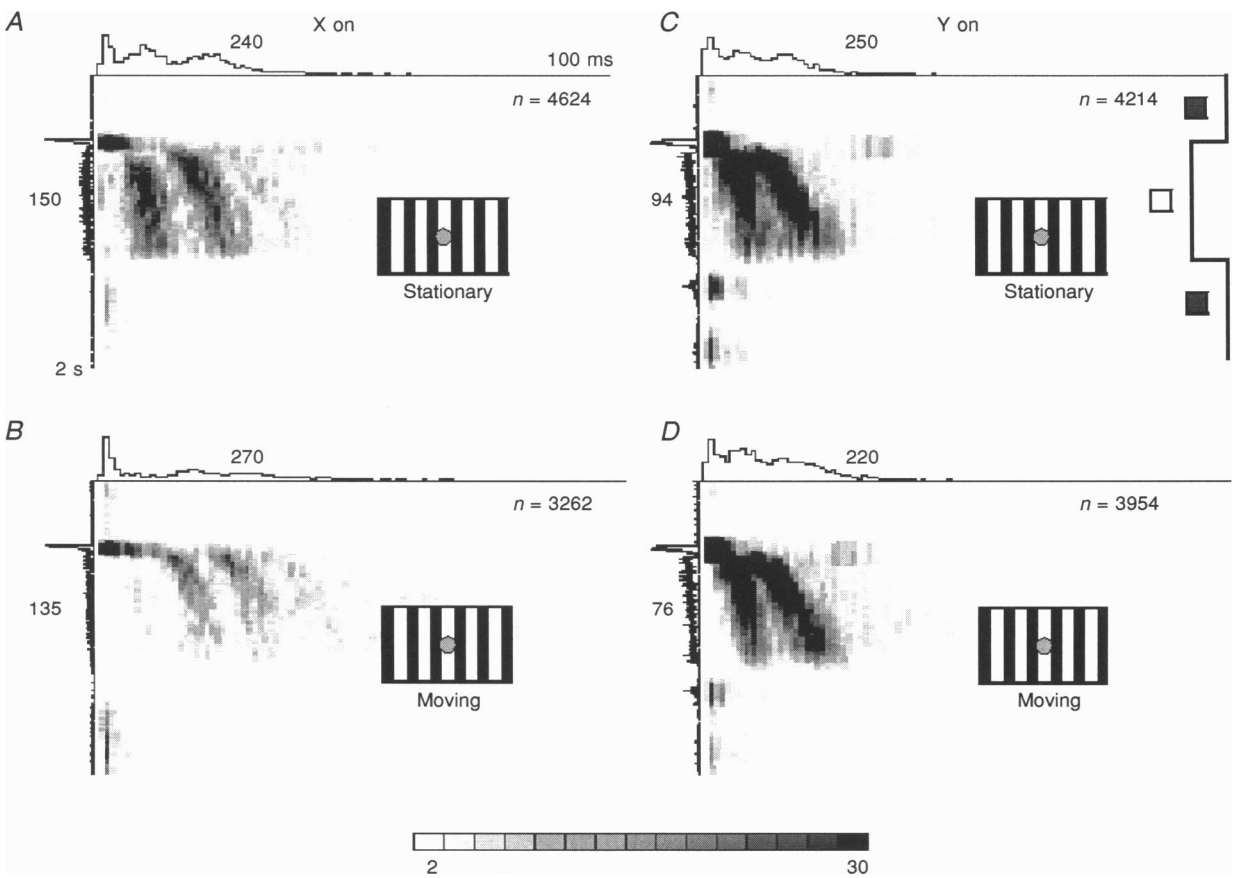

Figure 11. Effect of stimulating the periphery of the receptive field

Intervalograms for an X on-cell (*A* and *B*) and a Y on-cell (*C* and *D*), which demonstrate the different effects of an additional stimulation of the receptive field periphery by a moving grating in the background (rectangular contrast modulation of about 70%) on the response to the central spot of light (X, 1·2 deg; Y, 2·0 deg; 100%). The spot flashed on a stationary grating (*A* and *C*) elicits 3 and 2 bands in the X on- and the Y on-cell, respectively. With the moving grating in the background (*B* and *D*) the X-cell is strongly inhibited, which is predominantly accompanied by a redistribution of intervals to higher order bands and a total disappearance of the first band. In this case the bands are also slightly shifted to the left. The Y-cell is not affected by the moving grating and the interval distribution is not altered.

the retinal ganglion cell; (2) interval distribution of the retinal ganglion cell; (3) interneuron IPSP characteristic; and (4) interneuron interval distribution. In this setting it is not even necessary to assume a realistic shape for the synaptic potentials, so we have implemented the EPSP and IPSP shapes as triangular waves. The interval distributions are defined as γ-like distributions. The synaptic potentials are then added in a strictly linear way to yield the membrane potential of the modelled LGN cell. Spikes are elicited as soon as this membrane potential exceeds a certain threshold and summed interval distributions are computed for the LGN output (Fig. 14*A*). Note that intervalograms are not necessary to display the simulation results because the retinal firing frequency in the simulation is kept constant all the time. In reality, the firing rate of the tonic response can change during adaptation to the stimulus, but this effect is not essential for the model. Interval histograms are comparable with those obtained from the real cell responses at 800 ms on the time axis.

The panels in Fig. 14*B* show the resulting interval distributions as a function of the interneuron IPSP shape (width, varied vertically) and the average interneuron interval length (varied horizontally). All the activity will be eliminated as soon as the IPSPs are too wide and occur too often (top left). Frequent and small IPSPs (bottom left) as well as less frequent and wider IPSPs (top right) will, in this linear model, both result in a multimodal interval distribution showing three separate peaks in almost all cases. The most realistic transition from two to four peaks is found in the range of an IPSP width of 15–30 ms, occurring with a frequency of about 35–50 Hz. These parameters are well within the range of the fast IPSP input from LGN interneurons or perigeniculate neurons to LGN relay cells (Ahlsén, Lindström & Lo, 1985; Crunelli, Haby, Jassik-Gerschenfeld, Leresche & Pirchio, 1988; Mastronarde, 1992; Funke & Eysel, 1993). What should be noted in particular is that the multimodal patterns are very robust and that not even a high level of biophysical realism is necessary to achieve realistic-looking interval histograms, which also include those that show a dominance of the second or third interval peak, and not simply a monotonic decay of interval peaks of increasing order. The only critical parameter is the interval distribution of the retinal input. When the distribution is Poisson-like or γ-like, but

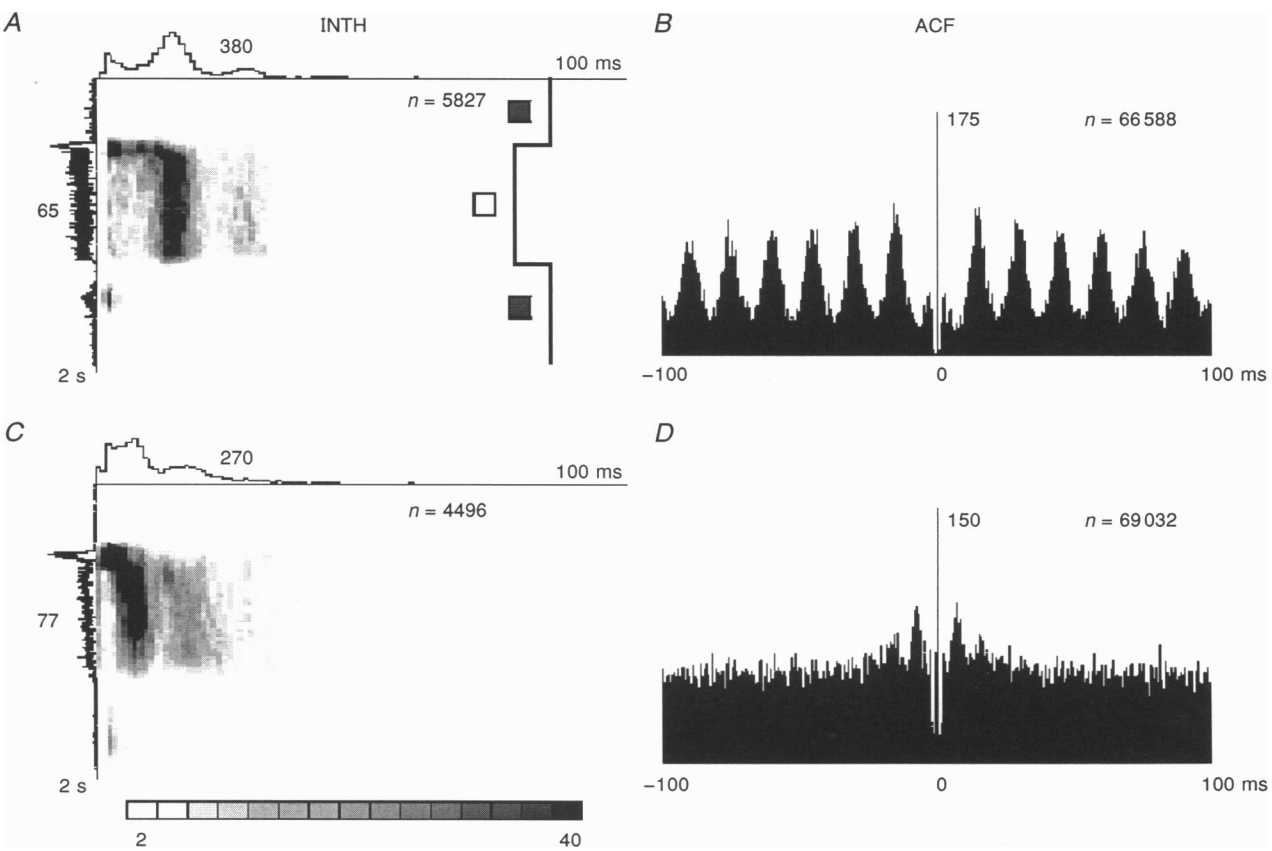

Figure 12. Intervalograms (*A* and *C*; INTH) and autocorrelation function (*B* and *D*; ACF) of 2 X on-cells

Both INTHs show one sharp and dominating interval band, but in *B* the autocorrelation function (ACF) shows a strong long-lasting oscillation with a frequency of 66·4 Hz, whereas in *D* there is no oscillation at all. Spot size, 1·5 deg in *A* and *B*, and 1·2 deg in the *C* and *D*; contrast modulation 100% for each.

broadly distributed around a fundamental interval of about 8 ms (range > 8 ms; compare with width at half-height in Figs 4*C* and *D*, and 5*E* and *F*), no multimodal distribution appears. The latter case would correspond to simulation of an off-cell (not shown).

A more interesting case arises from the convergence of several cells, each of which possesses a multimodal interval distribution. Figure 15*A* shows the connection scheme for a minimalistic convergence of LGN to cortex. In Fig. 15*B* the interval histograms and autocorrelation functions for a certain parameter combination are shown for the LGN cells. Multimodal distributions occur as in Fig. 14, and the autocorrelations show oscillations in the range of 30–50 Hz. Similar to the experimental observations, several decaying peaks are observed in the autocorrelation function. The cortical autocorrelation functions obtained from the simulations are shown in Fig. 15*C* for large changes in the interval ranges of the retinal input (vertically) and the inhibitory interneurons (horizontally). The diagram marked with the arrow represents the situation shown in Fig. 15*B*. Oscillations in the range of 30–90 Hz are clearly visible in all plots, with a few exceptions where they fade. Note that the rather large parameter variation probably exceeds the variability even of a group of adjacent LGN cells during similar stimulation. This implies that in a more realistic case the higher convergence onto the cortical cells, which leads to more response variability, might be counterbalanced by a less variable spiking pattern of the individual input cells.

DISCUSSION

Early results

First indications that cells in the visual system can produce multimodal interval distributions appeared in the article by Bishop, Levick & Williams (1964), in which they analysed spontaneous activity without stimulation. Their findings were supplemented by the results of Poggio & Viernstein (1964), who observed bimodal interval patterns in some spontaneously active lemniscal neurons. The use of visual stimuli is necessary in any attempt to decode the information processing mechanisms in the visual system. In most cases, however, the rather fast-changing spiking pattern of the cells during visual stimulation impairs the detection of a multimodal interval pattern. Based on well-

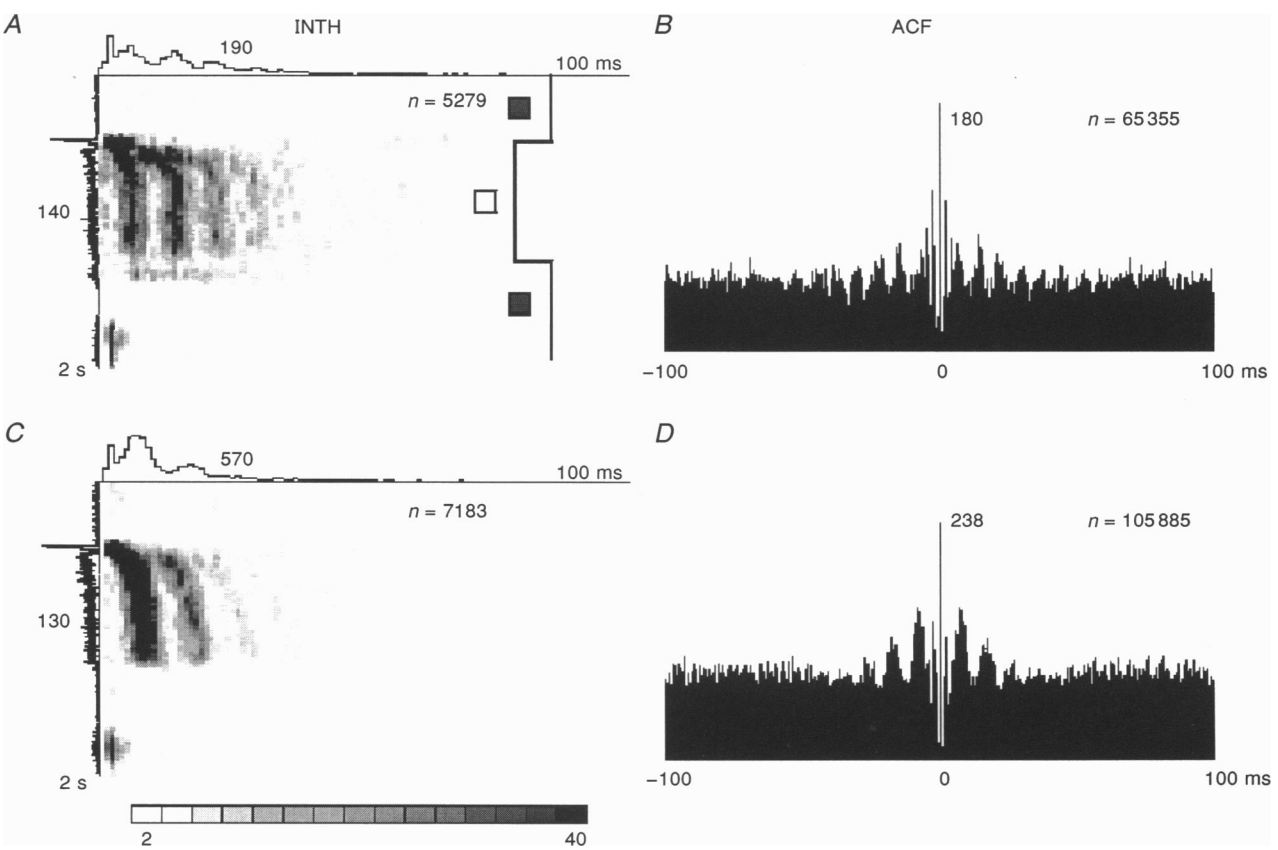

Figure 13. Intervalograms (*A* and *C*) and more typical ACFs (*B* and *D*) of 2 different X on-cells
(Compare Fig. 12.) Usually the ACFs show a short-lasting oscillation of 3–7 cycles, which lasts for about 30–50 ms. Spot size, 1·0 deg, with 100% contrast modulation for both cells. Frequencies of the short-lasting oscillations are 125·9 Hz (*B*) and 104·3 Hz (*D*).

known sliding window averaging methods in this context the novel implementation of the 'intervalogram' made it possible to visualize multimodal interval distributions also during stimulation. The fast adaptation characteristic of many cells in the visual and other systems emphasizes the advantage of this method in many experimental situations. It is also worth noting that such a sliding window evaluation process can be applied to many other standard neurophysiological analysis methods (e.g. auto- and cross-correlations).

The origin of multimodal interval patterns

In the course of presenting the results we have already introduced a rather simple mechanism, which we believe underlies the generation of interval bands (Fig. 6). Originally, this mechanism was suggested by Bishop *et al.* (1964), but they did not have clear evidence for its location. The simultaneous recording of retinal prepotentials and LGN cell spikes in the current study strongly suggests that the inhibitory agent acts at the level of the LGN and not before. Also in line with this argument are the studies that

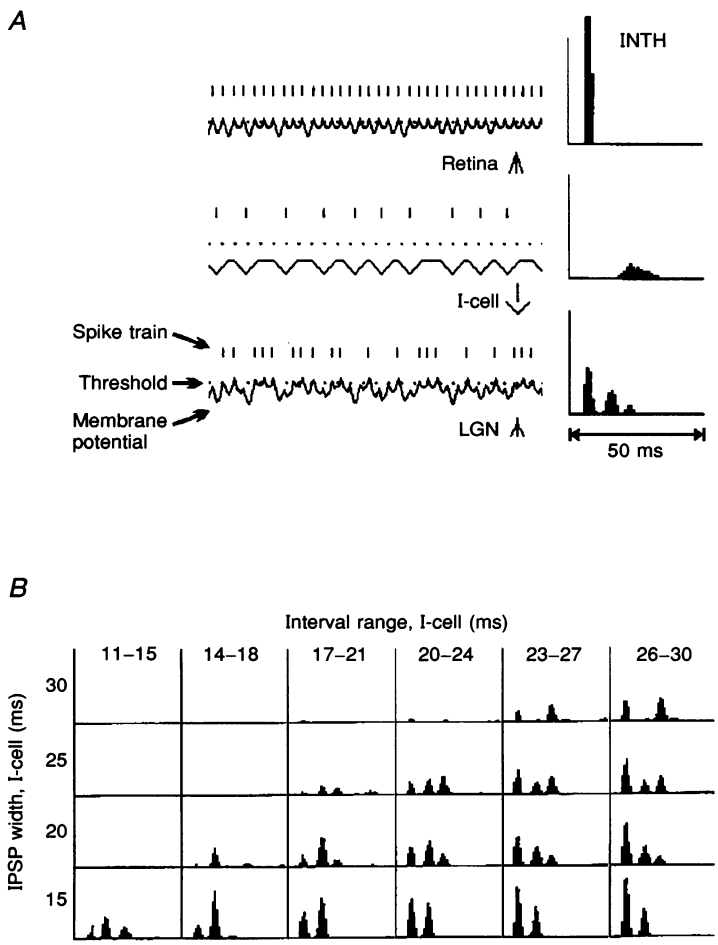

Figure 14. Schematic illustration of the simple LGN computer model (*A*) that reliably generates multimodal interval distributions (*B*) very similar to those found in the experimental data

A, the computer program generates spike trains for a retinal input and an intra-geniculate inhibitory input (I-cell) with a γ-like interval distribution in a certain range. INTHs to the right show the interval distributions. Retinal spike intervals are in the range of 6–10 ms, as found in the experimental data. Inputs are transformed to excitatory or inhibitory postsynaptic potentials at the LGN relay cell and summed in a linear way. LGN spikes are generated by suprathreshold depolarizations and the resulting multimodal interval distribution is shown in the bottom INTH of *A*. For simplicity, postsynaptic potentials were of triangular shape. The symbols to the right of the labels show the shape of the postsynaptic potentials and the vertical line indicates the difference between resting membrane potential and spike threshold, which has been set to 100%. The amplitude of a single postsynaptic potential was set to a fraction of this difference. *B*, sequence of LGN INTHs resulting from a simulation with different inhibitory inputs. The spike interval range (horizontal axis) and the IPSP width (vertical axis) were varied. Depending on the parameter combinations, the first, the second and even the third interval peak can dominate.

fail to show multimodal interval distributions in the retina (Kuffler *et al.* 1957; Rodieck, 1967; Troy & Robson, 1992). Physiological evidence can never be an ultimate proof for a connection between neurons. Nevertheless, several predictions arose from the simple connection scheme (Fig. 6) that could be verified. Gradual shifts in the firing frequency and inhibitory deletions are the two main effects that occur during the stimulus protocols that we used. A contrast reduction mainly leads to an interval *shift* as a consequence of the gradual reduction of the retinal mean firing rate. A change in stimulus size or a stimulation of the receptive field periphery, on the other hand, results in a *redistribution* of the intervals to the higher order bands as a result of the increasing inhibitory input, which increases more strongly in the LGN than in the retina (Sillito & Kemp, 1983; Cleland & Lee, 1985). Certain stimulus situations (e.g. changes in the level of adaptation and contrast) lead to a superposition of these two effects.

All our results can be interpreted most easily in terms of inhibition acting directly at the LGN cells and inducing the multimodal interval patterns. While this does not conclusively rule out other possible mechanisms, in addition, our computer simulations showed that no particular requirements are necessary to produce multimodal interval patterns so long as the parameters in the simulation remain within the physiological range. In fact, the scheme is unfortunately so robust that we cannot use the different parameter sets to conclude from whence this inhibition could originate. Possible candidates are the GABAergic interneurons of the LGN, or the perigeniculate (PGN) neurons.

Models

Several mathematical models have been suggested for the generation of multimodal interval patterns, all of which originate from the scheme of a 'deletion inhibition' devised by Bishop *et al.* (1964) that we have also adopted here. Most of these models use point processes for the generation of spikes to make them analytically treatable. In the simplest version, Ten Hoopen (1966) suggested that a sharply tuned process with a narrow Gaussian or γ-interval distribution should be inhibited by a Poisson-distributed process. While this suggestion also underlies the simulations of Bishop *et*

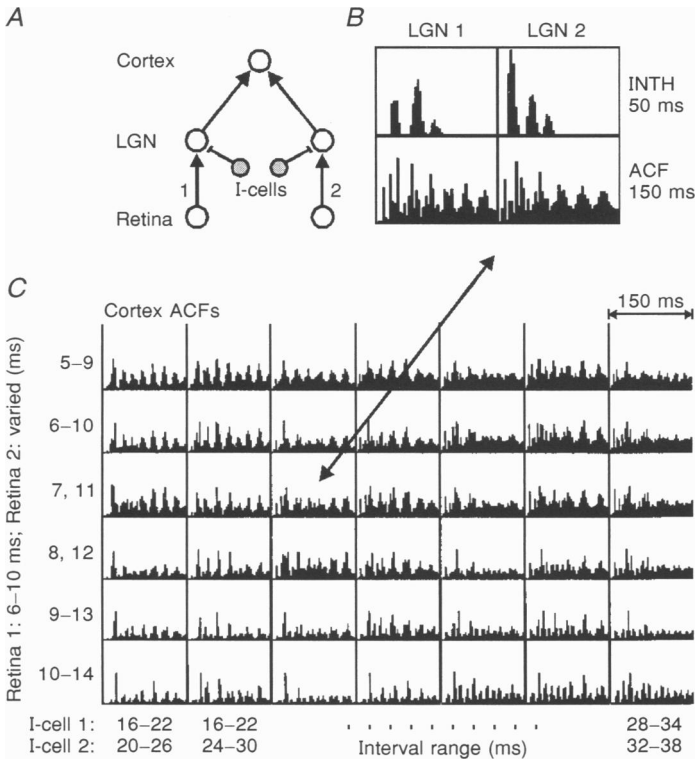

Figure 15. Oscillations in cortical ACFs obtained by a computer simulation that extends the simple model of Figs 6 and 14 by the convergence of two geniculate channels onto a cortical cell

The scheme of the connectivity is shown in *A*, the sequence of cortical ACFs in *C* and one example for the interval distributions and ACF patterns of the corresponding inputs of the two LGN cells in *B*. As shown in the schematic drawing (*A*), the geniculate circuitry consists of two identical but independent lines, which converge onto a single cortex cell. In line 1 the retinal interval range is fixed at 6–10 ms; in line 2 it changes systematically between 5–9 and 10–14 ms, as indicated on the left side in *C*. The interval ranges of both inhibitory inputs change stepwise (+4 ms, alternating) between 16–22 and 32–38 ms (bottom). Oscillations in a range of 30–90 Hz are visible in nearly all cortical ACFs as well as in the corresponding geniculate ACFs (see *B*).

al. (1964), Ten Hoopen & Reuver (1965) could solve it analytically. However, this apparently simple combination of two processes already leads to a rather intricate mathematical treatment. To avoid this level of complexity, van de Grind *et al.* (1971) suggested a mechanism that essentially used only the intrinsic refractory period of the nerve cells to generate multimodal interval patterns without any inhibitory convergence. While the mathematics of this model are more transparent, it is not supported by our experimental findings, which suggest the existence of inhibitory convergence.

The use of point processes in the models permits mathematical treatment. Unfortunately, however, narrow, point-like interactions without further assumptions will always lead to a monotone decrease in the height of the interval bands, in which the first interval band must dominate. This is easy to see in the following way. Assuming that the inhibitory interaction is restricted to a very narrow range (point) in time, then the height of the *first* interval band *following* the fundamental band is determined by the probability, $P_1 \leqslant 1{\cdot}0$, of a single inhibitory deletion in the target spike train. If the inhibitory process has no memory, then the probability of a second deletion anywhere in the spike train is independent of the first deletion. Thus, the probability of a second deletion directly after the first deletion, defined as P_2, is equal to the conditional probability: $P_2 = P_{\mathrm{del,del}} = P_1^2 \leqslant P_1 \leqslant 1{\cdot}0$. Defining the height of the fundamental interval band as 1·0, the height of the first following band is proportional to P_1 and the height of each following band, n, decreases monotonically with the nth power of P_1. (For a detailed treatment of this case see Ten Hoopen (1966), who also gives the correct values for the amplitude decrease of the modes.)

While earlier results (Bishop *et al.* 1964) showed such a decrease, our study demonstrates that the higher order bands can easily dominate (see Figs 3*A*, 8*A*, 10*B* and 11*B*), sometimes even accompanied by an almost total disappearance of the lower order bands (Figs 3*A* and 11*B*). Therefore, the assumption of a point process without memory must be dropped to acquire a more realistic description. One can assume a longer lasting (not point-like) inhibitory interaction (i.e. IPSP), again with Poisson interval distribution. Unfortunately, this describes a situation where the fundamental band will always dominate, which is not the case in many recordings.

There are two simple ways to achieve a more realistic model. First, one could assume that the inhibition is long lasting but shallow (e.g. like a modulatory effect), so that only the summation of every nth EPSP will lead to a spike in the LGN. Minor fluctuations in the level of the inhibition could alter the value n, leading to the observed interval distributions.

Alternatively, the combination of short to intermediately long IPSPs *and* a sharply tuned inhibitory interval distribution, as in our simple model, will generate all the observed cases. Support for this type of activity is given by intracellular studies that demonstrate rather short IPSPs in cat and rat relay cells (for example see Ahlsén *et al.* 1985; Crunelli *et al.* 1988) and by studies showing that local geniculate interneurons and PGN neurons are characterized by a long-lasting tonic activity (Mastronarde, 1992; Funke & Eysel, 1993). For PGN (or thalamic reticular) neurons, a preference for spike intervals occupying a narrow range has also been demonstrated (Pinault & Deschênes, 1992; Funke & Eysel, 1993). A broad interval range for the inhibitory input also produces multimodal interval distributions in the relay cells, but a clear dominance of higher order intervals (double or triple the length of the fundamental) is best achieved with a narrowly distributed inhibitory input.

This second alternative (short to intermediate IPSPs, narrow distribution) also has some interesting consequences. One of these is known as the 'high convergence effect' (van de Grind *et al.* 1971), i.e. pooling of many (> 5) narrowly distributed pulse sequences with random phases will yield an approximately Poisson-distributed output signal. We have just argued, however, that a Poisson-distributed inhibitory input to the LGN cells cannot exist, because this would always result is a monotone decay of the interval peaks. Provided our assumptions hold (short to intermediate IPSPs, narrow distribution), we can then conclude that either very few interneurons are involved in the generation of the inhibitory signal or, if many contribute, they have to fire in a rather synchronous pattern and with a similar sharply tuned interval distribution.

Thus, it becomes clear that this apparently trivial connectivity pattern (Fig. 6) already largely defies analytical calculation. Assuming a minimal degree of complication in the network, the above arguments and the computer simulations allow the following conclusions to be drawn: (1) interval band patterns cannot be attributed to a strict point process, but require IPSPs of a certain duration (10–30 ms); (2) the inhibitory interval distribution should be narrow; and (3) very few inhibitory interneurons probably account for the interval band pattern of each target cell.

Interval bands and oscillations

The temporal information in spike trains has become a central issue of research, particularly since the discovery of cortical oscillations in the 30–90 Hz range (Eckhorn *et al.* 1988; Gray *et al.* 1989). While many interpretations originally favoured a cortical origin of these oscillations, in the meantime it has become clear that subcortical structures could contribute to, or generate solely, such cortical oscillations (Bringuier *et al.* 1992; Ghose & Freeman, 1992; Nuñez, Amzica & Steriade, 1992; Pinault & Deschênes, 1992). Clear oscillatory patterns were observed by Ghose & Freeman (1992) only during spontaneous activity of the recorded LGN cells, but not during visual stimulation. The tonic activity of the ten example LGN cells that they showed is rather high (20–40 Hz) and could very well

correspond to the increased activity during static visual stimulation in our experience. The differences between these studies might, therefore, result from the different types of visual stimuli and the different methods used for the analysis of the spike trains. To establish oscillatory activity in an autocorrelogram, a rather constant firing pattern is needed for long periods. We have shown that this is found only during steady or slowly changing contrast, e.g. corresponding to quite low velocities of a moving stimulus (Gray, Engel, König & Singer, 1990). In addition, the intervalogram is more sensitive than spectral methods (e.g. autocorrelation) for the detection of a certain firing frequency that changes with time or contains spurious interruptions (see Fig. 3*D*, for the moving bar).

The simple simulation shown in Fig. 15 demonstrates that the observed interval pattern in the LGN in a most parsimonious way generates 30–90 Hz oscillations in a cortical target cell. The central requirement of this scheme is that the fundamental interval in the LGN is within a narrow range between 5 and 14 ms, which was experimentally observed in almost all stimulus situations (shifts of the fundamental interval with changing stimulus contrast). In addition, a certain number of inhibitory deletions must occur so that the second or third order bands also contribute to the activity in the LGN cells. This requirement is rather interesting from the viewpoint of a cortical cell. Cortical cells are almost always stimulated more efficiently with an elongated object and not with a small dot. Elongated stimuli, however, will always induce surround inhibition in the LGN cells and, hence, lead to a preponderance of the higher order interval bands in the response. Thus, an optimal stimulation of a cortical cell will always be one that fulfils the requirement of a high proportion of secondary intervals. It should also be noted that cortical oscillations are most efficiently induced with rather slow-moving stimuli (Gray *et al.* 1990) that would lead to a rather tonic response and, thus, to the expression of interval band patterns in the LGN. Also necessary to finally generate 40–60 Hz oscillations in the simulation is a smoothing of the originally rather sharp interval bands. This is a process which certainly occurs at each cortical cell as a consequence of the high input convergence and the statistical fluctuations of the spike trains. In our model, a convergence of only two cells was already sufficient to smooth the interval pattern and result in the desired oscillations. It is important to realize that similar oscillatory patterns were observed *for almost all realistic* parameter settings in the model. Regarding the wide range of oscillation frequencies observed in real cortical cells (30–90 Hz; Eckhorn *et al.* 1988; Gray *et al.* 1989) it becomes, therefore, more and more likely that the LGN input characteristic already suffices to induce cortical oscillations in the observed ranges, which could then be propagated to cells that do not receive direct LGN input. In reality, many more cells converge onto a cortical cell than just the two in the simulation. According to the arguments from above, this should result in the 'high convergence effect' and lead to a Poisson output distribution. A Poisson-distributed spike train, however, will not contain oscillatory patterns (Moore *et al.* 1966). This reasoning is apparently contradictory to the results of the simulation. So far, however, we have neglected the fact that a cortical cell relies on strong input summation before a spike is elicited. This high level of required coincidence waves the aforementioned 'high convergence effect', which only holds if each spike elicits a response. Therefore, a cortical cell will, in general, not produce a Poisson-distributed output from its many input signals, but rather will act as a coincidence detector ('coincidence scaler'; van de Grind *et al.* 1971). It has been shown that even with a multitude of Poisson inputs an ideal coincidence scaler would yield a γ-output (van de Grind *et al.* 1971). Thus, even with the high convergence onto a cortical cell, the resulting interval distribution can be sharp. Therefore, a high convergence is not necessarily contradictory to the suggested mechanism for the generation of cortical oscillations. A certain degree of synchronicity (coincidence) from the LGN, however, is necessary; otherwise the cortical cells would spike randomly or not at all. A synchronization process controlled by the corticofugal feedback has recently been demonstrated for the cat LGN (Sillito, Jones, Gerstein & West, 1994).

Differences in the on- and off-subsystems

Intriguingly, we found that mainly on-cells could produce interval bands, whereas off-cells respond in a less structured way. Commonly, on- and off-cells are regarded merely as sign-inverted components of a pulse-coded information-processing system to compensate for the lack of negative values for the impulse rates. This view neglects observed asymmetries between the systems, which go beyond a mere sign inversion.

We will first discuss findings from different areas (pharmacology and psychophysics), which support the possibility of a distinct difference between the on- and off-subsystems, before we turn to physiology and try to offer a possible explanation for the observed difference.

Pharmacologically, the on- and off-systems react differently at the level of the retinal bipolar cells, since on- and off-bipolar cells possess different types of glutamate receptor. The on-subsystem, but not the off-subsystem, can be efficiently blocked by 2-amino-4-phosphonobutyrate (Slaughter & Miller, 1981). This different receptor distribution may result in different mechanisms of spike generation.

Also, rather strong differences between the subsystems have been observed psychophysically. For example, a stimulus that is brighter than the background appears larger than a stimulus that is darker than the background (Weale, 1975). This is probably a spatially induced effect. Temporally induced effects, which could be based on the temporal differences in the activity of on- and off-cells

reported here, are also present. Using flicker stimuli, the darkness enhancement is greater than the brightness enhancement (Magnussen & Glad, 1975) and the threshold delays between the presentation of two adjacent lines in an apparent motion task are conceivably higher for dark lines than for bright lines (Wehrhahn & Rapf, 1992).

Physiologically, several observations also showed small differences in the receptive field characteristics of on- and off-cells even in the retina. For example, the average size of the receptive field of on-cells is smaller than that of off-cells (Hammond, 1974).

While all these reports from different disciplines seem indirectly to support the notion of a difference between the on- and off-systems, a more direct link can be found between the study of Troy & Robson (1992) and our findings. These investigators have shown that the interval distributions of retinal off-cells are more spread out and diffuse (i.e. more Poisson-like) than those of on-cells, which produce rather sharply tuned γ-distributions in most stimulus situations (Troy & Robson, 1992). While we have shown that the intervalograms of retinal prepotentials of on-cells are narrow (Fig. 9), we found that the distributions for off-cell prepotentials were always very broad (data not shown), fully in accordance with the findings of Troy & Robson (1992). In particular, this effect could very well underlie the different capabilities of on- and off-cells to produce interval bands in the LGN. Let us assume that a deletion mechanism exists (see Fig. 6) and that it is *identical* in its connectivity pattern for LGN on- and off-cells. The spike train of the retinal off-cells has a broad Poisson-like interval distribution and EPSPs will be deleted from such a spike train. This, however, will also result in a Poisson-like output interval distribution for the LGN cells, only with a longer 'tail', as has been shown analytically by Ten Hoopen (1966).

For the retinal on-cells, on the other hand, the interval distribution is narrow and the deletion mechanism can act as illustrated in Fig. 6 (see Ten Hoopen, 1966). Therefore, it seems as if the difference in the on- and off-subsystems is not necessarily based on a different intra-LGN connectivity pattern, but it could also stem from an amplification of small differences in the interval distributions already existing in the retina.

Functional considerations and speculations

The modification of the firing frequency with deletion inhibition effectively works like an AND gate with one inverted input (the inhibitory input). In this scheme the inhibition acts as a veto mechanism. Each input IPSP will totally block (i.e. veto) all incoming excitatory activity. Such a mechanism results in an effective gating of neuronal activity and emphasizes the function of the LGN as an active gate to the cortex. A veto mechanism as a result of the synaptic interaction via $GABA_A$ receptors at Cl^- channels has already been proposed (Koch, Poggio & Torre, 1983). While this mechanism relies on non-linear interactions at the cell membrane, in our model we have an example of a small neuronal circuit interacting in an entirely linear manner (e.g. Fig. 14), which also results in a divisive (i.e. non-linear) effect on the output firing rate. We have argued that probably only two (or very few) components are involved in the generation of the excitatory retinal input (Mastronarde, 1987) as well as the inhibitory deletion signal and both probably act close to the soma. Therefore, this small circuitry in the LGN seems to be an example in which linear summation is entirely sufficient to produce an output governed by a veto mechanism.

The resulting non-linear effect of the deletion inhibition can very efficiently downregulate the impulse rate of the target cell. To fire a cortical cell, summation of many inputs is necessary. The non-linear regulation of the firing frequency of the LGN cells could, therefore, act like a switch at the cortical target cell. A cortex cell would respond during only brief phases of rather optimal stimulation (i.e. without too many deletions) of a large fraction of its input cells. This also corresponds to the much more phasic behaviour of cortical cells compared with their LGN inputs. Therefore, the observed deletion inhibition seems to be an example of a signal flow regulation mechanism based in the LGN, which could in principle also be available to other thalamic substructures.

In the computer simulations we found that slight hyperpolarizing DC shifts of the membrane potential of the simulated LGN cells strongly increases the number of deletions (not shown). This indicates that global alterations of the membrane potential at the level of the LGN could also have a significant effect on the transmission rate between retina and cortex. We found that synchronization of the EEG causes a strong reduction of the tonic light response (Funke & Eysel, 1992) associated with a total disappearance of lower order interval bands (no. 1 + 2); at the same time higher order bands (up to no. 6) appear (not shown). The corticofugal feedback loop, which, to a large degree, seems to act nonspecifically on the global activity level of the LGN (see Funke & Eysel, 1992; but see also Sillito *et al.* 1994), could act as such a 'throughput regulator'. In particular, Curró Dossi, Nuñez & Steriade (1992) found a hyperpolarization of thalamocortical neurons of about 9 mV after elimination of the corticothalamic feedback, which favours a facilitatory cortical input to geniculate relay neurons. A tonic cortical input would cause some global effect, similar to that seen with changes in the EEG pattern or cortical cooling (Funke & Eysel, 1992), but a timely precise cortical input to LGN relay cells might be potent enough to prevent the deletion of single spikes, thereby supporting the synchronization of geniculate activity (Sillito *et al.* 1994). We are currently investigating this topic using reversible cortical inactivation.

ABELES, M. (1982). Role of cortical neuron: Integrator or coincidence detector? *Israel Journal of Medical Sciences* **18**, 83–92.

ADELSON, E. H. & BERGEN, J. R. (1991). The plenoptic function and the elements of early vision. In *Computational Models of Visual Processing*, ed. LANDY, M. S. & MOVSHON J. A., pp. 3–20. MIT Press, Cambridge, MA, USA and London.

AHLSÉN, G., LINDSTRÖM, S. & LO, F.-S. (1985). Interaction between inhibitory pathways to principal cells in the lateral geniculate nucleus of the cat. *Experimental Brain Research* **58**, 134–143.

ARIEL, M., DAW, N. W. & RADER, R. K. (1983). Rhythmicity in rabbit retinal ganglion cell responses. *Vision Research* **23**, 1485–1493.

BARLOW, H. B. & LEVICK, W. R. (1969). Changes in the maintained discharge with adaptation level in the cat retina. *Journal of Physiology* **202**, 699–718.

BISHOP, P. O., LEVICK, W. R. & WILLIAMS, W. O. (1964). Statistical analysis of the dark discharge of lateral geniculate neurones. *Journal of Physiology* **170**, 598–612.

BRINGUIER, V., FREGNAC, Y., DEBANNE, D., SHULZ, D. & BARANYI, A. (1992). Synaptic origin of rhythmic visually evoked activity in kitten area 17 neurones. *NeuroReport* **3**, 1065–1068.

CLELAND, B. G. & LEE, B. B. (1985). A comparison of visual responses of cat lateral geniculate nucleus neurones with those of ganglion cells afferent to them. *Journal of Physiology* **369**, 249–268.

CRUNELLI, V., HABY, M., JASSIK-GERSCHENFELD, D., LERESCHE, N. & PIRCHIO, M. (1988). Cl^-- and K^+-dependent inhibitory postsynaptic potentials evoked by interneurones of the rat lateral geniculate nucleus. *Journal of Physiology* **399**, 153–176.

CURRÓ DOSSI, R., NUÑEZ, A. & STERIADE, M. (1992). Electrophysiology of a slow (0·5–4 Hz) intrinsic oscillation of cat thalamocortical neurons *in vivo*. *Journal of Physiology* **447**, 215–234.

DAYHOFF, J. & GERSTEIN, G. L. (1983). Favoured patterns in spike trains. II. Application. *Journal of Neurophysiology* **49**, 1349–1363.

ECKHORN, R., BAUER, R., JORDAN, W., BROSCH, M., KRUSE, W., MUNK, M. & REITBÖCK, H. J. (1988). Coherent oscillations: a mechanism of feature linking in the visual cortex? *Biological Cybernetics* **60**, 121–130.

EYSEL, U. TH., GRÜSSER, O.-J. & HOFFMANN, K.-P. (1979). Monocular deprivation and the signal transmission by X- and Y-neurons of the cat lateral geniculate nucleus. *Experimental Brain Research* **34**, 521–539.

FISCHER, B. & KRÜGER, J. (1974). The shift effect in the cat's lateral geniculate neurons. *Experimental Brain Research* **21**, 225–227.

FUNKE, K. & EYSEL, U. T. (1992). EEG-dependent modulation of response dynamics of cat dLGN relay cells and the contribution of the corticogeniculate feedback. *Brain Research* **573**, 217–227.

FUNKE, K. & EYSEL, U. T. (1993). Modulatory effects of acetylcholine, serotonin and noradrenaline on the activity of cat perigeniculate neurons. *Experimental Brain Research* **95**, 409–420.

GHOSE, G. M. & FREEMAN, R. D. (1992). Oscillatory discharge in the visual system: does it have a functional role? *Journal of Neurophysiology* **68**, 1558–1574.

GRAY, C. M., ENGEL, A. K., KÖNIG, P. & SINGER W. (1990). Stimulus-dependent neuronal oscillations in cat visual cortex: receptive field properties and feature dependence. *European Journal of Neuroscience* **2**, 607–619.

GRAY, C. M., KÖNIG, P., ENGEL, A. K. & SINGER, W. (1989). Oscillatory responses in cat visual cortex exhibit inter-columnar synchronization which reflects global stimulus properties. *Nature* **338**, 334–337.

HAMMOND, P. (1974). Cat retinal ganglion cells: size and shape of receptive field centres. *Journal of Physiology* **242**, 99–118.

KAPLAN, E., MUKHERJEE, P. & SHAPLEY, R. (1993). Information filtering in the lateral geniculate nucleus. In *Contrast Sensitivity*, vol. 5, ed. SHAPLEY, R. & MAN-KIT LAM, D., pp. 183–200. MIT Press, Cambridge, MA, USA.

KAPLAN, E., PURPURA, K. & SHAPLEY, R. M. (1987). Contrast affects the transmission of visual information through the mammalian lateral geniculate nucleus. *Journal of Physiology* **391**, 267–288.

KOCH, C., POGGIO, T. & TORRE, V. (1983). Nonlinear interaction in a dendritic tree: localization, timing and role in information processing. *Proceedings of the National Academy of Sciences of the USA* **80**, 2799–2802.

KUFFLER, S. W., FITZHUGH, R. & BARLOW, H. B. (1957). Maintained activity in the cat's retina in light and darkness. *Journal of General Physiology* **40**, 683–702.

LAUFER, M. & VERZEANO, M. (1967). Periodic activity in the visual system of the cat. *Vision Research* **7**, 215–229.

MCCLURKIN, J. W., GAWNE, T. J., OPTICAN, L. M. & RICHMOND, B. J. (1991*a*). Lateral geniculate neurons in behaving primates. II. Encoding of visual information in the temporal shape of the response. *Journal of Neurophysiology* **66**, 794–808.

MCCLURKIN, J. W., OPTICAN, L. M., RICHMOND, B. J. & GAWNE, T. J. (1991*b*). Concurrent processing and complexity of temporally encoded neuronal messages in visual perception. *Science* **253**, 675–677.

MAGNUSSEN, S. & GLAD, A. (1975). Brightness and darkness enhancement during flicker: perceptual correlates of neuronal B- and D-Systems in human vision. *Experimental Brain Research* **22**, 399–413.

MASTRONARDE, D. N. (1987). Two classes of single-input X-cells in cat lateral geniculate nucleus. I. Receptive field properties and classification of cells. *Journal of Neurophysiology* **57**, 357–380.

MASTRONARDE, D. N. (1992). Nonlagged relay cells and interneurons in the cat lateral geniculate nucleus: Receptive-field properties and retinal inputs. *Visual Neuroscience* **8**, 407–441.

MOORE, G. P., PERKEL, D. H. & SEGUNDO, J. P. (1966). Statistical analysis and functional interpretation of neuronal spike data. *Annual Review of Physiology* **28**, 493–522.

NUÑEZ, A., AMZICA, F. & STERIADE, M. (1992). Intrinsic and synaptically generated delta (1–4 Hz) rhythms in dorsal lateral geniculate neurons and their modulation by light-induced fast (30–70 Hz) events. *Neuroscience* **51**, 269–284.

PINAULT, D. & DESCHÊNES, M. (1992). Voltage-dependent 40 Hz oscillations in rat reticular thalamic neurons in vivo. *Neuroscience* **51**, 245–258.

POGGIO, G. F. & VIERNSTEIN, L. J. (1964). Time series analysis of impulse sequences of thalamic somatic sensory neurons. *Journal of Neurophysiology* **27**, 517–545.

RODIECK, R. W. (1967). Maintained activity of cat retinal ganglion cells. *Journal of Neurophysiology* **30**, 1043–1071.

SILLITO, A. M., JONES, H. E., GERSTEIN, G. L. & WEST, D. C. (1994). Firing induced by feedback from the visual cortex. *Nature* **369**, 479–482.

SILLITO, A. M. & KEMP, J. A. (1983). The influence of GABAergic inhibitory processes on the receptive field structure of X- and Y-cells in cat dorsal lateral geniculate nucleus (dLGN). *Brain Research* **277**, 63–77.

SINGER, W. (1977). Control of thalamic transmission by corticofugal and ascending reticular pathways in the visual system. *Physiological Reviews* **57**, 386–420.

SLAUGHTER, M. M. & MILLER, R. F. (1981). 2-Amino-4-phosphonobutyric acid: A new pharmacological tool for retina research. *Science* **211**, 182–184.

SOMPOLINSKY, H., GOLOMB, D. & KLEINFELD, D. (1990). Global processing of visual stimuli in a neural network of coupled oscillators. *Proceedings of the National Academy of Sciences of the USA* **87**, 7200–7204.

TEN HOOPEN, M. (1966). Multimodal interval distributions. *Kybernetik* **3**, 17–24.

TEN HOOPEN, M. & REUVER, H. A. (1965). Selective interaction of two independent recurrent processes. *Journal of Applied Probability* **2**, 286–292.

TROY, J. B. & ROBSON, J. G. (1992). Steady discharges of X and Y retinal ganglion cells of cat under photopic illuminance. *Visual Neuroscience* **9**, 535–553.

VAN DE GRIND, W. A., KOENDERINK, J. J., VAN DER HEYDE, G. L., LANDMAN, H. A. A. & BOUMAN, M. A. (1971). Adapting coincidence scalers and neural modeling studies of vision. *Kybernetik* **8**, 85–105.

VON DER MALSBURG, C. (1981). The correlation theory of brain function. Internal Report 81–2, Department of Neurobiology, MPI for Biophysical Chemistry, Göttingen, FRG.

WEALE, R. A. (1975). Apparent size and contrast. *Vision Research* **15**, 949–955.

WEHRHAHN, C. & RAPF, D. (1992). ON- and OFF-pathways form separate neural substrates for motion perception: psychophysical evidence. *Journal of Neuroscience* **12**, 2247–2250.

Acknowledgements

We would like to thank E. Nelle for critical comments on the manuscript and B. Bendmann and V. Onasch for technical assistanee during the experiments. This work was supported by the Deutsche Forschungsgemeinsschaft WO-388/4-1.

Received 2 September 1994; accepted 13 December 1994.